Frequency Domain Equalization and Multiuser Detection Techniques for DS-UWB Systems

by

Praveen Kaligineedi

B.Tech, Indian Institute of Technology, Kanpur, 2004

A THESIS SUBMITTED IN PARTIAL FULFILMENT OF THE REQUIREMENTS FOR THE DEGREE OF

Master of Applied Science

in

The Faculty of Graduate Studies

(Electrical and Computer Engineering)

The University of British Columbia

August 2006

Abstract

Ultra wideband (UWB) is an emerging technique for high data rate transmissions over short distances. Direct sequence (DS)-UWB approach is one of the two competing high data rate UWB standards, along with multiband orthogonal frequency division multiplexing (OFDM). One of the major challenges in a DS-UWB receiver design is the intersymbol interference (ISI). Several time domain equalization schemes to eliminate ISI have been proposed in the literature for DS-UWB systems. However, for long dispersive channels, these time domain equalization schemes require very high computational complexity in order to achieve desired bit error performance. Frequency domain equalization schemes which give better performance than time domain equalization schemes for single carrier systems, over highly dispersive channels, are well known in the literature. In this thesis, performances of frequency domain minimum mean square error (MMSE) linear, decision feedback and iterative decision feedback equalizers are studied for uncoded single user BPSK and 4BOK DS-UWB systems. We compare bit error rate (BER) performance of various time domain and frequency domain equalization techniques and evaluate their computational complexity. We show that the frequency domain equalization techniques can offer better trade off between complexity and performance compared to the time domain equalization techniques for DS-UWB systems. We then consider frequency domain multiuser detection techniques for DS-UWB systems. We employ frequency domain successive interference cancelation and parallel interference cancelation schemes combined with frequency domain equalization schemes and study their average BER performance. We derive low complexity frequency domain MMSE turbo equalization schemes for coded BPSK and 4BOK DS-UWB systems. Soft interference cancelation is used in the multiuser systems to remove multiple access interference (MAI). The average BER performance is obtained using simulations. The performance gain due to turbo equalization is shown to be significant, particularly, for DS-UWB systems with lower spreading gain. The improvement in the performance due to turbo detection is found to be very high for multiuser systems.

Table of Contents

List of Tables

List of Figures

List of Symbols

M'	:	constellation size
M	:	number of symbols in a data block
N_s	:	spreading factor
C	:	set of bi-orthogonal codes
$p(t)$	:	transmitted pulse shape
$c_{tr}^{i}[\cdot]$	:	bi-orthogonal code transmitted during i^{th} symbol period
$s'[\cdot]$	:	block chip sequence obtained at the transmitter after spreading and chip interleaving
L_p	:	length of prefix
$s^m[\cdot]$	:	m^{th} block chip sequence obtained at the transmitter after adding prefix
$x(t)$	:	transmitted signal
$h_p(t)$	:	continuous time passband channel impulse response
$h(t)$	:	continuous time baseband channel impulse response
f_c	:	carrier frequency
α_l	:	multipath gain
τ_l	:	multipath delay
$h[\cdot]$	:	discrete time channel impulse response
L_s	:	length of discrete channel impulse response $h[\cdot]$
$z(t)$	:	continuous time additive white Gaussian noise
$z[\cdot]$	:	discrete time additive white Gaussian noise
N_0	:	power spectral density of additive Gaussian noise
σ_2	:	noise variance
$r^m(t)$	:	continuous time received signal corresponding to data block m
$r^m[\cdot]$	:	discrete time received signal corresponding to data block m
$S(n)$	:	discrete Fourier transform of $s[k]$
$Z(n)$	:	discrete Fourier transform of $z[k]$
$H(n)$	:	discrete Fourier transform of $h[k]$

$Y(n)$	:	frequency domain output of the forward filter
$y[\cdot]$	:	inverse discrete Fourier transform of $Y(n)$
$Y^q(n)$	:	frequency domain output of the forward filter at the q^{th} iteration
$y^q[\cdot]$	:	inverse discrete Fourier transform of $Y^q(n)$
$E(\cdot)$	:	expected value operator
J	:	metric to be minimized
$W^q(n)$	:	feedforward filter at q^{th} iteration
$B^q(n)$	:	feedback filter at q^{th} iteration
J^q	:	metric to be minimized at q^{th} iteration
$\hat{S}^q(n)$	:	DFT of the estimated chip sequence after q^{th} iteration
σ_S^2	:	variance of the sequence $S(n)$
ν	:	decision feedback correction factor
X	:	the log normal shadowing factor of the channel impulse $h(t)$
L_c	:	total number of clusters in UWB channel model
N_c	:	total number of rays in each cluster in UWB channel model
L	:	number of symbols in the cyclic prefix for symbol based MMSE and MMSE-DFE
$d[\cdot]$	:	transmitted information bits
N_{fb}	:	number of feedback filter taps in symbol FD-DFE
$b[\cdot]$	:	feedback filter taps in symbol FD-DFE
N_r	:	number of rake fingers
N_f	:	number of forward filter taps in rake MMSE and rake MMSE-DFE receivers
N_b	:	number of feedback filter taps in rake MMSE-DFE receiver
P	:	total number of iterations for iterative DFE equalizer
U	:	number of users
$d_u[\cdot]$	:	u^{th} user data sequence
A_u	:	amplitude of user u at the receiver
$h_u(t)$	:	continuous time channel impulse response of user u
$h_u[\cdot]$	:	discrete time channel impulse response of user u
$s'_u[\cdot]$	:	u^{th} user block chip sequence obtained at the transmitter after spreading and chip interleaving
$s_u[\cdot]$	:	u^{th} user block chip sequence obtained at the transmitter after adding prefix
$x_u(t)$	:	transmitted signal of user u
$S_u(n)$	:	discrete Fourier transform of $s_u[k]$

$\sigma^2_{S_u}$	:	variance of the sequence $S_u(n)$
$H_u(n)$	:	discrete Fourier transform of $h_u[k]$
X_u	:	the log normal shadowing factor of the channel impulse $h_u(t)$
$W^{p,q}(n)$	:	feedforward filter at q^{th} equalization iteration and p^{th} PIC iteration
$B^{p,q}(n)$	:	feedback filter at q^{th} equalization iteration and p^{th} PIC iteration
$\tilde{d}^c[\cdot]$	:	uninterleaved coded channel bits
$d^c[\cdot]$	:	interleaved coded channel bits
$L_c(\cdot)$	:	log likelihood ratio generated by decoder
$L_e(\cdot)$	:	log likelihood ratio generated by equalizer
$Y_u^q(n)$	:	frequency domain output of the forward filter for u^{th} user and q^{th} iteration
$y_u^q[\cdot]$	:	inverse discrete Fourier transform of $Y_u^q(n)$
σ^2_{inter}	:	variance of the interference
E_b	:	Energy per user symbol

List of Abbreviations

AWGN	:	additive white Gaussian noise
BER	:	bit error rate
BPSK	:	binary phase shift keying
CDMA	:	code division multiple access
DEINT	:	deinterleaver
DFE	:	decision feedback equalization
DFT	:	discrete Fourier transform
DS	:	direct sequence
FD	:	frequency domain
FDE	:	frequency domain equalization
FEC	:	forward error correction
FFT	:	fast Fourier transform
FH	:	frequency hopping
IDFT	:	inverse discrete Fourier transform
IFFT	:	inverse fast Fourier transform
INT	:	interleaver
IR	:	impulse radio
ISI	:	intersymbol interference
IT-DFE	:	iterative decision feedback equalization
LLR	:	log likelihood ratio
LOS	:	line-of-sight
MAI	:	multiple access interference
MAP	:	maximum *a* posteriori
MB	:	multi-band
MBOK	:	M-ary biorthogonal keying
MMSE	:	minimum mean square error
NLOS	:	non line-of-sight
OFDM	:	orthogonal frequency division multiplexing

PIC	:	parallel interference cancelation
PLL	:	phase locked loop
PN	:	pseudorandom noise
P/S	:	parallel-to-serial conversion
QPSK	:	quaternary phase shift keying
RF	:	radio frequency
SC	:	single carrier
SIC	:	successive interference cancelation
SISO	:	soft input soft output
SNR	:	signal to noise ratio
SOVE	:	soft-output Viterbi equalizer
S/P	:	serial-to-parallel conversion
UNII	:	unlicensed national information infrastructure
UWB	:	ultra wideband
WPAN	:	wireless personal area networks

Acknowledgement

First and foremost, I would like to thank my supervisor, Prof Vijay K. Bhargava, for his guidance, encouragement and support. I would like to thank Chandika for clarifying all my doubts and contributing valuable insights to my thesis work. I would like to thank the instructors of my graduate courses for helping me obtain a good understanding of the basic concepts. Finally, I would like to thank all members of our lab for their support and for providing a stimulating and fun environment in which to learn and grow.

Chapter 1

Introduction

In recent years, rapid development has been observed in wireless personal area networks (WPAN). WPAN connects devices within reach of an individual, using radio waves. Typical range of a WPAN is 1- 10m. WPAN is used to connect computer and its peripherals such as printer, keyboard, mouse, joystick etc, various personal digital assistants (PDAs) and portable computers without using cables. WPAN uses cheap low power devices. Working group 15 of IEEE LAN/MAN standards committee developed various standards for WPAN. Task group 1 of this working group (802.15) deals with Bluetooth technology. Task group 3 and 4 deal respectively with high data rate and low data rate WPANs based on ultra wideband (UWB) technology.

Bluetooth is a standard for short range, low power and low cost wireless communication [2]. Bluetooth devices use unlicensed spectrum in 2.4 GHz band and have a range of 1m to 100m. It achieves data rates up to 3 Mbps. Even though Bluetooth has been widely deployed and provides cheap short distance communication, there are still certain key challenges with Bluetooth which need to be addressed. Bluetooth suffers from interference from other devices operating in 2.4 GHz band [3]. This interference could severely limit the performance of Bluetooth devices as 2.4 GHz band is getting overcrowded very rapidly, partly due to Bluetooth devices themselves. Another major disadvantage of Bluetooth is that the data rates provided are not sufficient for high data rate multimedia applications.

UWB achieves much higher data rates than Bluetooth at very low transmit power levels due to its large unlicensed bandwidth. UWB systems transmit signals with bandwidth greater than 500MHz or fractional bandwidth greater than 0.2 at all times [1]. The Federal Communications Commission (FCC) has allocated 7.5GHz of unlicensed spectrum in the 3.1GHz to 10.6GHz frequency band for the use of UWB devices [4]. UWB bandwidth is enough to effectively stream multiple simultaneous high-quality video streams. Its low power consumption improves the battery life of the portable devices. Moreover, UWB technology requires less complex hardware as the transmission takes place in baseband eliminating the need for mixers, RF oscillators or PLLs which are necessary in narrowband systems. Thus, UWB technology is cost effective and UWB devices are more compact. Due to its low spectral density, unlicensed UWB radio emissions do not add up to cause harmful interference to other radio systems operating in dedicated bands.

1.1 DS-UWB vs MB-OFDM

Presently, there are two competing UWB technologies used for high data rate wireless personal area networks (WPAN). One of them is the direct sequence (DS)-UWB [5] which is based on DS-code division multiple access (CDMA) technology and the other is multi-band orthogonal frequency division multiplexing (MB-OFDM) [6] which is based on OFDM technology.

In DS-UWB system, the total available spectrum is divided into two sub-bands: a lower band (3.1-4.85 GHz) and a higher band (6.2-9.7 GHz). The use of UNII bands (5.15-5.35 GHz and 5.725-5.825 GHz) is intentionally avoided to prevent interference between UWB and the existing IEEE 802.11a devices. A DS-UWB signal consists of a train of very short pulses with duration in the order of fractions of nanoseconds. The information is carried in the amplitude and/or polarity of the pulses. Multiple access capability is achieved using DS-CDMA technique. A rake receiver can be used for a DS-UWB system to take advantage of the high multipath diversity of the indoor channel. DS-UWB can achieve data rates in excess of 1Gbps. DS-UWB devices are lower in cost compared to MB-OFDM devices. However, the short symbol duration of the DS-UWB signal leads to intersymbol interference (ISI), especially, at high data rates. So, an equalizer is necessary to compensate ISI for high data rate DS-UWB systems.

In a MB-OFDM system, the total spectrum is divided into 5 band groups. Each band is further divided into subbands with bandwidth 528 MHz. A block of transmit data is scrambled, encoded, interleaved, and quaternary phase shift keying (QPSK) modulated to form a OFDM symbol. These OFDM symbols are transmitted over different subbands determined by a pre-defined frequency hopping (FH) pattern. The use of OFDM makes the system robust to ISI, eliminating the need for a complex equalizer. OFDM can also exploit the frequency diversity inherent in multipath channels, when combined with error control coding and interleaving. MB-OFDM can achieve data rates up to 480 Mbps. However, MB-OFDM systems were found to be more sensitive to timing and frequency synchronization errors than DS-UWB systems [7].

1.2 Equalization for DS-UWB systems

A typical UWB channel consists of a large number of realizable multipath components. Typically, in case of multipath channels, a rake receiver is used to yield diversity gain from the multipaths, taking advantage of the good correlation properties of the spreading sequences. However for DS-UWB systems, at high data rates or correspondingly low spreading gains, the performance of the rake receiver is degraded due to presence of ISI. Hence, it becomes necessary to use an equalizer in the receiver to eliminate ISI. Various equalization schemes have been proposed in the literature for DS-UWB systems. In [8], [9] the performance of various linear and decision feedback time domain equalization schemes for DS-UWB systems were investigated. Application of widely linear processing to equalization was proposed in [9]. In [10], a suboptimal linear MMSE equalizer which exploits the sparse nature of the UWB channel to decrease the computational complexity was studied. However, the complexity of these equalization techniques could still be very high for severely dispersive UWB channels, in order to achieve a desired performance. A decision feedback equalization scheme based on energy detector was proposed in [11]. This scheme avoids estimation of the path amplitudes and delays and is less sensitive to synchronization errors. However, it leads to degradation in the bit error performance.

1.3 SC-FDE

Frequency domain equalization (FDE) techniques were shown to offer performance similar to time domain equalization techniques at much lower complexity for single carrier (SC) systems over strong frequency selective channels [12]. SC systems with FDE are very similar in structure to a OFDM system. Fig 1.1 shows a SC system employing FDE and an OFDM system. However, SC systems with FDE exhibit certain advantages over an OFDM system. SC systems with FDE have lower peak to average power ratio. Thus, it has significantly lower RF front end costs compared to OFDM system. SC-FDE systems are more robust to phase noise and frequency offsets due to close frequency spacing of its subcarriers and therefore, have less stringent oscillator requirements compared to OFDM.

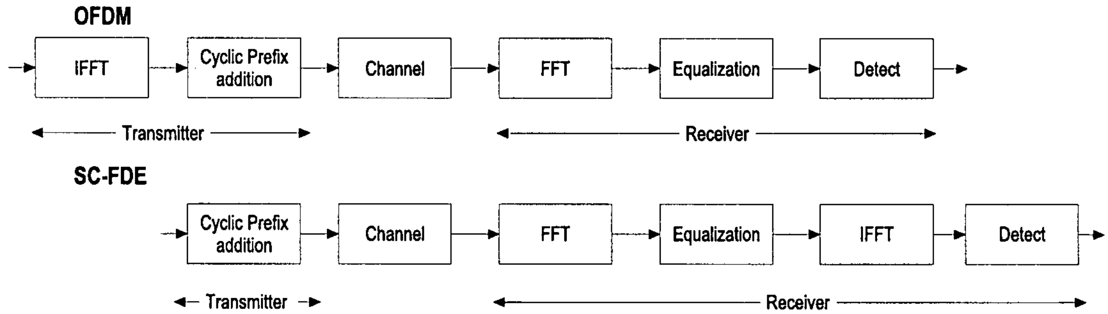

Figure 1.1: Comparison of OFDM and SC-FDE system

A frequency domain linear equalizer was first investigated for SC-FDE systems in [25]. SC-FDE as an alternative to multicarrier systems was studied in [24]. Frequency domain Decision feedback equalization in which the feedforward filter is applied in frequency domain and feedback filter is applied in time domain was investigated in [12]. In [26], a decision feedback equalizer in which both feedforward and feedback filter operate in frequency domain was proposed. This was applied for DS-CDMA systems in [17]. Recently a frequency domain minimum mean square error (FD-MMSE) equalization scheme was proposed for DS-UWB and IR-UWB systems and was shown to have better performance compared to MMSE-Rake receiver [14], [15]. Time-division multiple-access (TDMA) scheme for the binary phase-shift keying (BPSK) SC-FDE DS-UWB systems was proposed in [16]. Frequency domain multiuser detection schemes have been investigated for DS-CDMA systems in [17].

1.4 Turbo Equalization

Initially, turbo equalization was considered using full-state trellis based soft equalizers (e.g., the soft-output Viterbi equalizer (SOVE) in [20], the maximum *a posteriori* (MAP) algorithm based equalizer and its suboptimal variants in [21]). Unfortunately, full-state trellis based soft equalizers may be highly computationally-expensive for long channels and/or for large signal constellations. Later, MMSE-based iterative equalization schemes were proposed in e.g., [31]. In MMSE-based schemes, the MAP algorithm based equalizer (or a suboptimal trellis based soft equalizer) found in the original version of turbo equalization schemes is replaced with a combination of soft ISI cancelation and linear MMSE-based filtering. Because of low-complexity, MMSE-based turbo equalization is much more attractive to be employed in practical mobile receivers compared to MAP-based turbo equalization. In [28], a turbo equalization scheme in which the equalizer operates in frequency domain was proposed for single carrier systems. This significantly reduces the computational complexity, especially, for highly dispersive channels.

1.5 Thesis Outline

In this thesis, we adapt various frequency domain linear and non-linear equalization and multiuser detection schemes for MBOK DS-UWB systems and analyze their performance. We compare BER performances and corresponding complexities of various time domain and frequency domain equalization schemes for single user uncoded BPSK DS-UWB systems and show that frequency domain equalization schemes can provide better trade off between performance and complexity compared to time domain schemes.

Frequency domain turbo equalization schemes for single user coded SC systems have been investigated in [28], [33] and [27]. In this thesis, we extend these results for BPSK and 4BOK DS-UWB for both single user and multiuser scenarios and investigate their performance.

This thesis is organized as follows. In Chapter 2, we consider uncoded single user MBOK DS-UWB system. We present the frequency domain linear MMSE equalizer and iterative frequency domain decision feedback equalizers (FD-DFE) for MBOK DS-UWB systems. Then, we present symbol based frequency domain equalization schemes for BPSK and 4BOK DS-UWB systems. Computational complexities of various equalizers are evaluated and simulation results are presented.

In Chapter 3, we consider frequency domain multiuser detection schemes, viz., parallel interference cancelation (PIC) and successive interference cancelation (SIC) for uncoded multiuser DS-UWB systems. In Chapter 4, we consider coded DS-UWB systems. We derive frequency domain turbo equalization schemes for BPSK and 4BOK DS-UWB systems and evaluate their BER performance. Conclusions are finally drawn in Chapter 5.

Chapter 2

Frequency Domain Equalization

2.1 Introduction

Frequency domain equalization techniques were shown to offer better trade off between performance and complexity compared to time domain equalization techniques, for single carrier systems with severe channel dispersions [12]. In this chapter, we employ frequency domain equalization techniques for single user MBOK DS-UWB systems. We investigate both linear and non-linear frequency domain equalization techniques [17]. We also define chip based equalization schemes and symbol based equalization schemes for MBOK DS-UWB systems. The complexity of these equalization schemes is compared with that of time domain equalization schemes.

2.2 System model

2.2.1 Transmitter

We consider a single-user DS-UWB system employing M'-ary Bi-Orthogonal Keying (M'-BOK) and short ternary codes. A M'-BOK system maps $\log_2 M'$ bits into a bi-orthogonal ternary code of length N_s. The bi-orthogonal code is selected from an assigned code set $C = \{c_1, c_2, ..., c_{\frac{M'}{2}}, -c_1, -c_2, ..., -c_{\frac{M'}{2}}\}$ where $c_1, c_2, ..., c_{M'/2}$ are orthogonal to each other [5].

The transmit signal of a M'-BOK DS-UWB system is given by

$$
\begin{aligned}
x(t) &= \sum_{i=-\infty}^{\infty} \sum_{j=0}^{N_s-1} c_{tr}^{i}[j] p(t - iT_s - jT_c) \\
&= \sum_{k=-\infty}^{\infty} s'[k] p(t - kT_c)
\end{aligned}
\tag{2.1}
$$

where $\{c_{tr}^{i}[j]\}_{j=0}^{j=N_s-1} \in C$ represents the ith transmitted data symbol and has unit energy. N_s denotes the spreading factor. T_c is the chip duration and $T_s = N_s * T_c$ is the symbol duration. $p(t)$ is the unit energy transmit pulse of time duration T_c and $s'[iN_s + j] = c_{tr}^{i}[j]$.

In a system employing FDE, the data symbols are transmitted in blocks. In order to apply FDE, the convolution of the channel impulse response and data signal must be circular. This circularity can be achieved in two ways [13].

First method is to attach a cyclic prefix to the block of data i.e. for every MN_s data samples we take last L_p data samples and attach them at the beginning. Thus transmit block m contains

$$
\begin{aligned}
s^m &= [s^m[0], s^m[1], s^m[2], ..., s^m[MN_s + L_p - 1]] \\
&= [s'[mMN_s + MN_s - L_p + 1], s'[mMN_s + MN_s - L_p + 2], \\
&\quad ..., s'[mMN_s + MN_s - 1], s'[mMN_s], s'[mMN_s + 1], \\
&\quad ..., s'[mMN_s + MN_s - 1]]
\end{aligned}
$$

The other method is to append a pseudo random sequence $pn[i]_{i=0}^{L_p-1}$ to the data samples [12]. In this case the transmit block m is given by

$$
\begin{aligned}
s^m &= [s^m[0], s^m[1], s^m[2], ..., s^m[MN_s + L_p - 1]] \\
&= [s'[mMN_s], s'[mMN_s + 1], ..., s'[mMN_s + MN_s - 1], \\
&\quad pn[0], pn[1], ..., pn[L_p - 1]]
\end{aligned}
\tag{2.2}
$$

Moreover, a PN sequence is transmitted before transmission of first data block. For

M'-BOK, we transmit information regarding $M \log_2 M'$ bits in each block.

2.2.2 Channel Model

UWB channel model proposed for IEEE 802.15.3a standard has been considered [22]. The IEEE 802.15.3a UWB channel model is a modification of the Saleh-Valenzuela [23] multipath channel model. The interarrival time of multipath components is exponentially distributed. Moreover, the multipath arrivals are grouped into two different categories: a cluster arrival and a ray arrival within a cluster. The amplitudes of the multipaths are lognormal distributed. The model also includes a lognormal shadowing term to account for total received multipath energy variation that results from blockage of the line-of-sight path.

The passband physical multipath channel can be represented as

$$h_p(t) = \sum_{k=0}^{N_c-1} \sum_{l=0}^{L_c-1} \alpha'_{k,l} \cdot \delta(t - T_l - \tau_{k,l}) \tag{2.3}$$

where L_c represents the total number of clusters, N_c represents the total number of rays in the cluster. T_l is the cluster arrival time and $\tau_{k,l}$ is the arrival time of the k^{th} ray in l^{th} cluster. T_l and $\tau_{k,l}$ are exponentially distributed. $\alpha'_{k,l}$ is multipath gain of k^{th} ray in l^{th} cluster. The magnitude of $\alpha'_{k,l}$ is lognormal distributed. The amplitude of the multipath component is multiplied with +1 or -1 with equal probability to account for signal inversion. The total energy in the multipath components is normalized to one. Finally, X models the lognormal shadowing.

Model parameters were designed to fit the measurement results. 4 different channel models have been proposed for 4 different scenarios: CM1 channel model for line-of-sight (LOS) (0-4m) channel measurements, CM2 channel model for non LOS (NLOS) (0-4m) channel measurements, CM3 channel model for NLOS (4-10m) channel measurements and CM4 channel model for extreme NLOS multipath channel.

The above multipath channel model (2.3) can be expressed in simplified form as follows

$$h_p(t) = \sum_{l=0}^{L-1} \alpha_l \cdot \delta(t - \tau_l) \tag{2.4}$$

L denotes the number of multipath components, α_l and τ_l are, respectively, the path gain and the delay associated with the lth path. We assume that channel is quasi-static i.e the channel impulse response within a block is constant.

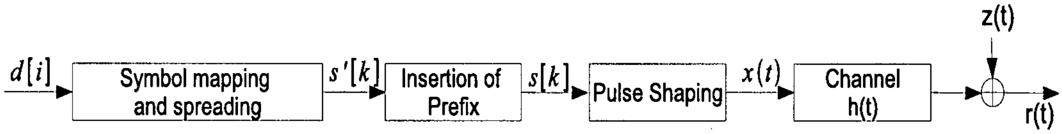

Figure 2.1: Transmitter and channel for single user DS-UWB system

The baseband equivalent of the passband channel model (2.4) is given by

$$h(t) = \sum_{l=0}^{L-1} \alpha_l e^{-j2\pi f_c \tau_l} \cdot \delta(t - \tau_l) \tag{2.5}$$

where f_c is the carrier frequency.

2.2.3 Receiver

The received baseband signal corresponding to m^{th} block is given by

$$r^m(t) = \sum_{l=0}^{L-1} \alpha_l e^{-j2\pi f_c \tau_l} \sum_{k=0}^{MN_s+L_p-1} s^m[k]p(t - kT_c - \tau_l) + z(t) \tag{2.6}$$

where $z(t)$ is complex zero mean additive white gaussian noise with variance σ^2.

After chip matched filtering and sampling at the chip rate, the discrete time received baseband signal is given by

$$r^m[k] = \sum_{l=0}^{L_s-1} h[l]s^m[k-l] + z[k] \quad k = 0, 1, ..., MN_s + L_p - 1 \tag{2.7}$$

where $h[l] = p(t) \otimes h(t) \otimes p^*(-t)|_{lT_c}$ and $z[k] = p^*(-t) \otimes z(t)|_{kT_c}$. Since only one block is processed at a time, hereafter, we omit the block index m. Transmitter and channel for single user DS-UWB is shown in Fig 2.1.

2.3 Linear MMSE equalization

For a DS-UWB system employing linear MMSE equalizer, a cyclic prefix of length L_p is attached at the transmitter. At receiver, the received samples corresponding to the cyclic prefix ($k = 0, 1, ..., L_p - 1$) are removed and discrete fourier transform is applied to the rest to obtain

$$R(n) = \sum_{l=0}^{MN_s-1} e^{-\frac{j2\pi ln}{MN_s}} r[L_p + l] \cdot \quad n = 0, 1, ..., MN_s - 1 \tag{2.8}$$

Similarly, we obtain DFTs $S(n)$, $Z(n)$ and $H(n)$ of $s[k]$, $z[k]$ and $h[k]$ respectively. Assuming that the length of the impulse response of the channel is less than L, the received signal can be expressed in frequency domain as follows

$$R(n) = H(n)S(n) + Z(n) \qquad n = 0, 1, ..., MN_s - 1 \tag{2.9}$$

Fig 2.2 shows the structure of the receiver employing linear MMSE equalization. R(n) is multiplied with MMSE filter coefficients $W(n)$ yielding

$$Y(n) = W(n)R(n) \qquad n = 0, 1, ..., MN_s - 1 \tag{2.10}$$

The MMSE equalizer minimizes the metric

$$J = \frac{1}{(MN_s)^2} \sum_{n=0}^{MN_s-1} E\left[|Y(n) - S(n)|^2\right] \tag{2.11}$$

Assuming that $\{S(n)\}_{n=0}^{MN_s-1}$ are independent and identically distributed, the filter coefficients minimizing the above metric (2.11) are given by

$$W(n) = \frac{H^*(n)}{N_s\sigma^2 + |H(n)|^2} \qquad n = 0, 1, ..., MN_s - 1 \tag{2.12}$$

The resultant output $Y(n)$ is converted to time domain signal $y[k]$ using inverse DFT (IDFT). The decision device, shown in Fig 2.3, then detects the symbol based on the time domain signal $y[k]$. The decision device forms the correlation of $y[k]$ with $c_1, c_2, ..., c_{\frac{M'}{2}}$ and decides in favor of the component with largest magnitude taking into consideration the sign of the component.

2.4 Iterative MMSE DFE

In [17], an iterative FD MMSE-DFE was proposed for DS-CDMA which attains a better performance than linear FD equalizers. In iterative MMSE DFE, an FD-MMSE forward filter is applied during the first iteration. Hard symbol estimates are obtained from filter outputs through IFFT, chip deinterleaving, despreading and

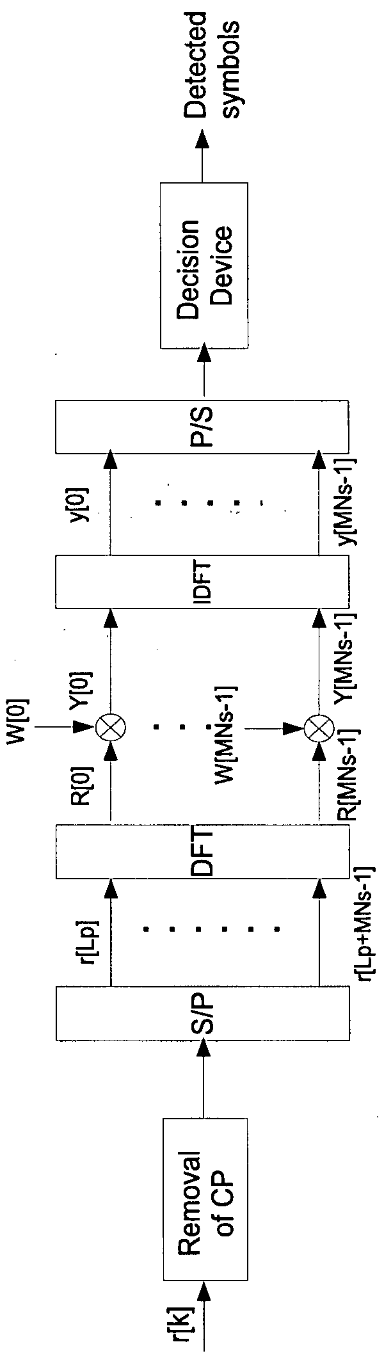

Figure 2.2: Frequency domain MMSE equalizer for a MBOK DS-UWB system

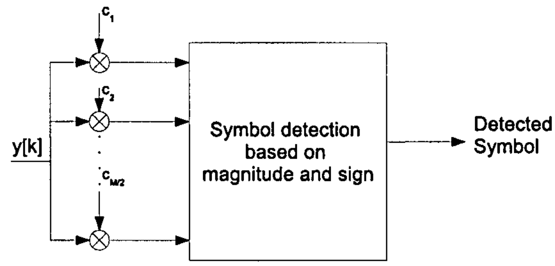

Figure 2.3: Decision device for a MBOK system

threshold detection. These detected symbols are then spread, chip interleaved and converted into frequency domain to obtain an estimate of the frequency domain chip sequence $S(n)$. This estimate is then fed back to obtain new symbol estimates based on MMSE criterion. This process is performed iteratively. Iterative MMSE-DFE equalization can achieve better performance than linear MMSE filter and MMSE-DFE at the cost of higher computational complexity.

In a DS-UWB system employing iterative FD-DFE, a PN sequence of length L_p is appended to the data block. DFT of the entire block of length $N = MN_s + L_p$ is taken. It was shown in [17] that interleaving the chip sequence before addition of cyclic performance leads to an improvement in system performance. Therefore, a chip interleaver is used at the transmitter after spreading. Correspondingly, a chip deinterleaver is introduced at the receiver.

Structure of iterative FD-DFE is shown in Fig 2.4. The output after $q = 1, 2, ..., Q$ iterations is given by [17]

$$Y^q(n) = W^q(n)R(n) + B^q(n)\hat{S}^{q-1}(n) \tag{2.13}$$

where $W^q(n)$ and $B^q(n)$ is feedforward filter and feedback filters respectively for q^{th} iteration. $\hat{S}_n^{q-1}$ is detected data at $q-1^{th}$ iteration.

The feedforward and feedback filter are chosen so as to minimize the following mean square error metric at q^{th} iteration [17]

$$J^q = \frac{1}{N^2}\sum_{n=0}^{N-1} E\left[|W^q(n)R(n) + B^q(n)\hat{S}^{q-1}(n) - S(n)|^2\right] \tag{2.14}$$

Frequency domain chip sequence $\{S(n)\}_{n=0}^{n=N-1}$ is assumed to be independent and

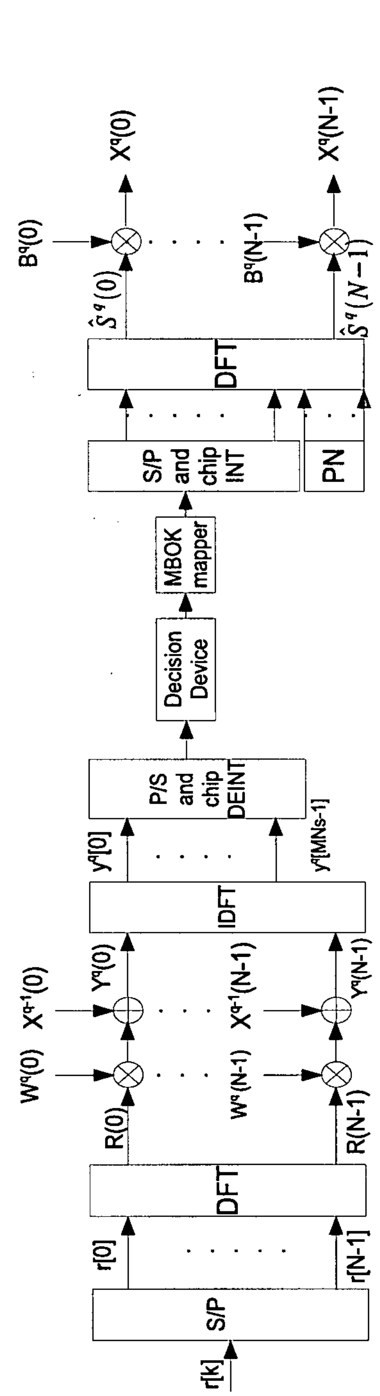

Figure 2.4: Iterative frequency Domain MMSE DFE for a MBOK DS-UWB system

identically distributed with mean zero and variance σ_S^2. Now, the average energy of chip sample for time domain signal $s[k]$ is $E(|s[k]|^2) = \frac{1}{N_s}$ (as energy per symbol is chosen as 1), $E(|S(n)|^2) = NE(|s[k]|^2) = \frac{N}{N_s}$. Since mean of $S(n)$ is zero, $\sigma_S^2 = E(|S(n)|^2) = \frac{N}{N_s}$. We further impose the condition on feedback filter [17]

$$\sum_{n=0}^{N-1} B^q(n) = 0 \tag{2.15}$$

so that the feedback filter does not remove the desired component. Minimizing the metric J^q under condition (2.15), yields the following feedforward filter at q^{th} iteration (see Appendix A) [17]

$$\begin{aligned} W^q(n) &= \frac{\sigma_S^2 H(n)^*}{N\sigma^2 + \sigma_S^2(1 - |\rho^q|^2)|H(n)|^2} \\ &= \frac{H(n)^*}{N_s\sigma^2 + (1 - |\rho^q|^2)|H(n)|^2} \end{aligned} \tag{2.16}$$

where ρ^q represents the correlation between the vectors $\hat{S}^{q-1}$ and S.

The feedback filter at q^{th} iteration is given by [17]

$$B^q(n) = -\rho^q \left[H(n)W^q(n) - \gamma^q\right] \tag{2.17}$$

where

$$\gamma^q = \frac{1}{N}\sum_{n=0}^{N-1} H(n)W^q(n) \tag{2.18}$$

In [17], following estimate for the correlation has been proposed.

$$\rho^q = \frac{\nu}{E_S}\sum_{n=0}^{N-1} \frac{R(n)}{H(n)} \hat{S}^{q-1}(n)^* \tag{2.19}$$

where $\nu \leq 1$ is a correction factor to reduce decision feedback error propagation and $E_S = \sum_{n=0}^{N-1} |S(n)|^2$.

However, this estimate of ρ^q is not accurate in case of UWB channels due to presence of spectral nulls. So we propose a new estimate of the correlation to overcome this problem. It is as follows

$$\rho^q = \frac{\nu}{E_S}(1 + \frac{\sigma^2 N_s}{X^2}) \sum_{n=0}^{N-1} \frac{R(n)H(n)^*}{\frac{1}{N_s}|H(n)|^2 + \sigma^2} \hat{S}^{q-1}(n)^* \tag{2.20}$$

where X represents the log normal shadowing factor of the channel impulse $h(t)$. The above estimate of ρ^q is found to be more accurate than the estimate in (2.19).

2.5 Symbol based Equalizers

2.5.1 BPSK system

For BPSK DS-UWB system, the bi-orthogonal code can be expressed as

$$c_{tr}^i[j] = d[i]c[j] \tag{2.21}$$

where $d[i]$ is the transmitted bit and $c[j]$ is the spreading sequence. Thus, in case of BPSK, knowledge of the spreading sequence of the user can be used in the equalizer. Symbol based equalization schemes make use of the knowledge of the spreading sequence to minimize the optimization metric [18]. For symbol based equalization schemes, instead of attaching a cyclic prefix or PN sequence of length L_p to the chip sequence, a prefix or PN sequence of length L is attached to the BPSK symbol sequence and then spreading is performed over the resultant symbol sequence.

MMSE Equalization

In case of symbol based MMSE equalizer, a cyclic prefix of length L is attached to the symbol sequence, before spreading, at the transmitter. The samples corresponding to cyclic prefix are removed at the receiver and DFT is taken of the block of size MN_s.

The symbol based MMSE filter minimizes the metric [18]

$$J = \sum_{i=0}^{M-1} E\left[|\tilde{d}[i] - d[i]|^2\right] \tag{2.22}$$

where $\tilde{d}[i]$ is the filter output.

The symbol based MMSE equalizer coefficients minimizing (2.22)are given by [18]

$$W(n) = \frac{H(n)^*}{\sigma^2 + \frac{|\hat{H}(n)|^2}{N_s}} \qquad n = 0, 1, ..., MN_s - 1 \tag{2.23}$$

where

$$|\hat{H}(n)|^2 = \sum_{k=0}^{N_s-1} |H(n+kM)_{\text{ mod } MN_s} C(n+kM)_{\text{ mod } MN_s}|^2 \tag{2.24}$$

The complexity to design the symbol based MMSE equalizer is higher compared to chip based MMSE equalizer presented in Section 2.3. However, the BER performance of symbol based MMSE equalization is better compared to BER performance of chip based MMSE equalization.

MMSE-DFE

The structure of the symbol based FD MMSE-DFE is shown in Fig 2.5. A PN symbol sequence is appended to the data symbol block. At the receiver, DFT is taken of the entire block of size $N' = (M + L)N_s$. The feedforward filter is implemented in frequency domain and feedback filter is implemented in time domain. FD MMSE-DFE also minimizes the metric (2.22). The feedforward filter minimizing the metric (2.22) is given by [18]

$$W(n) = \frac{H(n)^*[1 + \sum_{i=1}^{N_{fb}} b[i] e^{-\frac{j2\pi li}{M'}}]}{\sigma^2 + |\hat{H}(n)|^2} \qquad n = 0, 1, ..., N' - 1 \tag{2.25}$$

where $M' = M + L$, $\{b[i]\}_{i=1}^{N_{fb}}$ represent the feedback filter taps and

$$|\hat{H}(n)|^2 = \sum_{k=0}^{N_s-1} |H(n+kM')_{\text{ mod } N'} C(n+kM')_{\text{ mod } N'}|^2 \tag{2.26}$$

and $C(n)$ is the DFT of $c[j]$.

Optimal feedback filter taps of length can be obtained by solving following set of equations.

$$\mathbf{Vb} = -\mathbf{v} \tag{2.27}$$

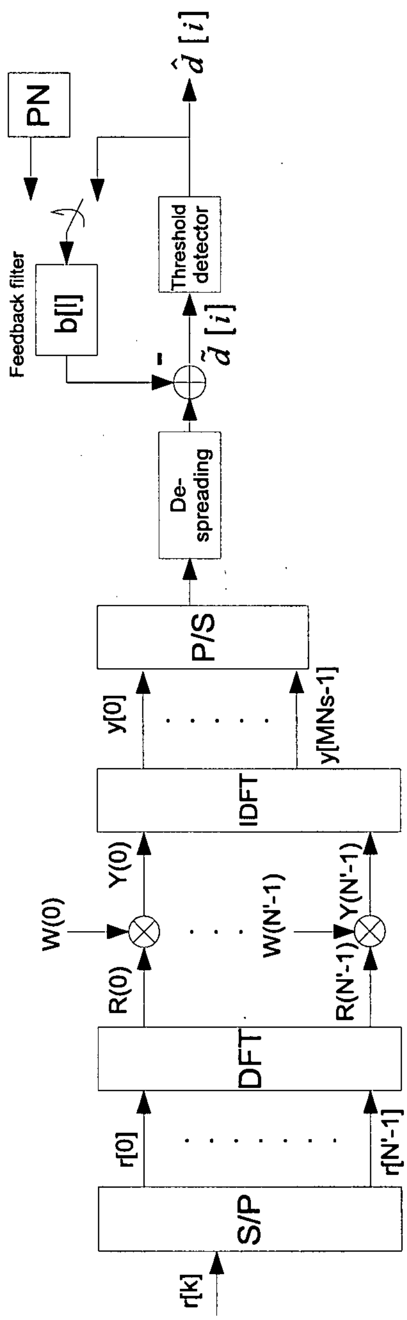

Figure 2.5: Symbol based frequency domain MMSE DFE for a BPSK DS-UWB system

where

$$\mathbf{V}(l,k) = \sum_{n=0}^{M+L-1} \frac{e^{-\frac{j2\pi(l-k)n}{M+L}}}{\sigma^2 + |\hat{H}(n)|^2} \tag{2.28}$$

$$\mathbf{v}(k) = \sum_{n=0}^{M+L-1} \frac{e^{-\frac{j2\pi kn}{M+L}}}{\sigma^2 + |\hat{H}(n)|^2} \tag{2.29}$$

for $1 \leq l, k \geq N_{fb}$. Design of optimal MMSE-DFE equalizer involves solving a set of linear equations (2.27) and thus, has high complexity.

Nevertheless, symbol based equalizers give better performance for BPSK systems because the assumption made by chip based equalizers that frequency domain sequence is independent and identically distributed makes them suboptimal.

2.5.2 4BOK system

In this section a single user 4BOK system using gray coding is considered. Let c_1 and c_2 be the two orthogonal spreading codes used for spreading. In Gray coding, the bits are mapped to spreading sequences as shown in Table 4.1. The transmitted

Table 2.1: Gray coding for 4BOK DS-UWB system

bits	Spreading Sequence
[-1 -1]	c_1
[-1 1]	c_2
[1 1]	$-c_1$
[1 -1]	$-c_2$

signal of above 4BOK system can be expressed as

$$
\begin{aligned}
x'(t) &= \sum_{i=-\infty}^{\infty} \sum_{j=0}^{N_s-1} c_{tr}^i[j] p(t - iT_s - jT_c) \\
&= \sum_{i=-\infty}^{\infty} \sum_{j=0}^{N_s-1} \left\{ d[2i] \left(-\frac{c_1[j] + c_2[j]}{2} \right) + d[2i+1] \left(\frac{-c_1[j] + c_2[j]}{2} \right) \right\} p(t - iT_s - jT_c) \\
&= \sum_{i=-\infty}^{\infty} \sum_{j=0}^{N_s-1} \{ d[2i]\tilde{c}_1[j] + d[2i+1]\tilde{c}_2[j] \} p(t - iT_s - jT_c) \qquad (2.30) \\
&= \sum_{k=-\infty}^{\infty} \{ \tilde{s}_1'[k] + \tilde{s}_2'[k] \} p(t - kT_c) \qquad (2.31) \\
&= \sum_{k=-\infty}^{\infty} s'[k] p(t - kT_c)
\end{aligned}
$$

where $\tilde{c}_1[j] = -\frac{c_1[j]+c_2[j]}{2}$, $\tilde{c}_2[j] = \frac{-c_1[j]+c_2[j]}{2}$, $\tilde{s}_1'[iN_s + j] = d[2i]\tilde{c}_1[j]$ and $\tilde{s}_2'[iN_s + j] = d[2i+1]\tilde{c}_2[j]$.

At the receiver, after matched filtering and chip rate sampling, we have

$$
r[k] = \sum_{l=0}^{L_s-1} h[l]s[k-l] + z[k] = \sum_{l=0}^{L_s-1} h[l]\{\tilde{s}_1[k-l] + \tilde{s}_2[k-l]\} + z[k] \qquad k = 0, 1, ..., MN_s + L_p - 1 \qquad (2.32)
$$

where $\tilde{s}_1$ and $\tilde{s}_2$ are obtained from $\tilde{s}_1'$ and $\tilde{s}_2'$ respectively by adding corresponding cyclic prefixes.

So a single user 4BOK system can be considered as 2-user BPSK system employing orthogonal spreading sequences. Now, symbol based equalizers can be applied assuming bits $\{d[2i]\}_{i=0}^{M/2}$ to be bits of user 1 with spreading sequence $\tilde{c}_1[j]$ and $\{d[2i+1]\}_{i=0}^{M/2}$ to be bits of user 2 with spreading sequence $\tilde{c}_2[j]$. We apply MMSE and MMSE-DFE filters for each user, treating the other user to be an independent white Gaussian interference.

2.6 Computational Complexity

Computational complexities of the various frequency and time domain equalizers for BPSK DS-UWB systems are shown in Table 2.1 and 2.2. Table 2.1 presents the processing complexity of the equalizer. Table 2.2, presents the order of computational complexity of equalizer design.

Table 2.2: Computational complexity of the receiver per output symbol for BPSK system

Equalizer	No. of complex multi. per detected symbol
Rake	$N_r N_s$
Rake MMSE	$N_r N_s + N_f$
Rake DFE	$N_r N_s + N_f$
FD MMSE	$N_s \log_2 MN_s$
FD-IT-DFE	$Q\frac{N}{M}\log_2 N$ $+(2Q-1)N_s$
symbol FD-MMSE	$N_s \log_2 MN_s$
symbol FD-DFE	$\frac{N}{M}\log_2 N + N_{fb}$

Table 2.3: Complexity of equalizer design per block for BPSK system

Equalizer	Order of complexity
Rake MMSE	$O\left((N_f+L)^2\right)$
Rake DFE	$O\left((N_f+L)^2\right)$
FD MMSE	$O(MN_s)$
FD-IT-DFE	$O(QN)$
symbol FD MMSE	$O(MN_s)$
symbol FD-DFE	$O(N_{fb}^2 + \frac{N_{fb}}{2}\log_2 N_{fb}$ $+\frac{N}{2}log_2 N)$

2.7 Simulation Results

We consider BPSK and 4BOK DS-UWB systems using ternary spreading sequences of length $N_s = 12$ and $N_s = 6$. We simulate the BER performance for CM4 channel model [22]. A root raised cosine function with roll off factor 0.3 is used as the pulse shape. We consider transmission in lower band (3.1-4.85 GHz). The chip rate is chosen to be 1313 MHz and the center frequency f_c is 3939 MHz [5]. We assume complete channel information at the receiver.

For BPSK systems, the following ternary spreading codes are used [5]

$$\begin{aligned} N_s = 12 &\longrightarrow \frac{1}{\sqrt{11}}[0 -1 -1 -1\ 1\ 1\ 1 -1\ 1\ 1 -1\ 1] \\ Ns = 6 &\longrightarrow [1\ 0\ 0\ 0\ 0\ 0] \end{aligned}$$

For 4BOK system, we use following ternary spreading codes [5]

$$N_s = 12 \quad \longrightarrow \quad \begin{array}{l} [1\,0\,0\,0\,0\,0\,0\,0\,0\,0\,0\,0] \\ [0\,0\,0\,0\,0\,0\,1\,0\,0\,0\,0\,0] \end{array}$$

For frequency domain equalization, number of data symbols per block is $M = 256$ and length of prefix or appended PN sequence is $L_p = 255$. The decision feedback correction factor ν is chosen to be 1. In case of symbol based FD-DFE for BPSK systems, we have chosen PN sequence length $L = 31$ for $N_s = 12$ and $L = 63$ for $N_s = 6$. The number of feedback filter taps is taken as $N_{fb} = \lceil \frac{L_s}{N_s} \rceil$. For symbol based FD-MMSE we have chosen length of channel prefix as $L = 22$ for $N_s = 12$ and $L = 44$ for $N_s = 6$. The total number of iterations for FD iterative DFE is represented by Q. $N_0 = \sigma^2$ is used to denote the power spectral density of the additive Gaussian noise. E_b is the average recieved energy per bit.

We also simulate the time domain equalizers proposed in [9], we choose number of rake fingers $N_r = 16$. N_f and N_b represent the number of feedforward and feedback filter taps, respectively, of rake DFE receiver. N_f also represents number of MMSE filter taps in rake MMSE receiver. Performance of the chip level MLSE receiver is also shown.

In Table 2.3 and 2.4, we present the numerical values of the computational complexities for various time and frequency domain equalizers for a BPSK DS-UWB system with $N_s = 6$. The parameters used in these tables for computing the numerical values correspond to the receivers whose BER performance is shown in Fig 2.6.

We can see from Tables 2.3, 2.4 and Fig 2.6 that the frequency domain equalizers offer better performance than time domain equalization techniques at a much lower complexity especially at low signal-to-noise ratios (SNRs).

Fig 2.7 and Fig 2.8 show the BER performance of the frequency domain equalization techniques for BPSK DS-UWB systems and 4BOK DS-UWB systems, respectively, with spreading factor $N_s = 12$. Fig 2.9 shows the BER performance of the frequency domain equalization techniques for 4BOK DS-UWB systems with spreading factor $N_s = 6$. Fig 2.10, shows the performance gain due to chip interleaving before addition of the prefix for 4BOK system with $N_s = 6$. We see that the gain is substantial.

Symbol based frequency domain equalizers were found to exhibit better perfor-

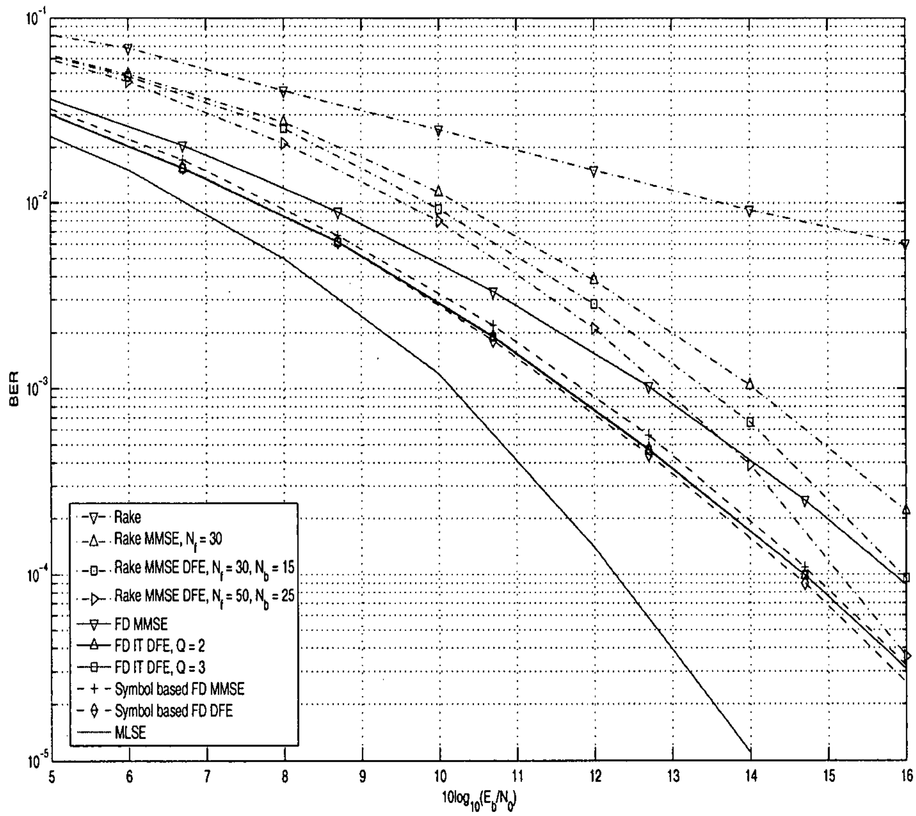

Figure 2.6: BER performance of various time domain and frequency domain equalizers for a BPSK UWB system with spreading factor $N_s = 6$

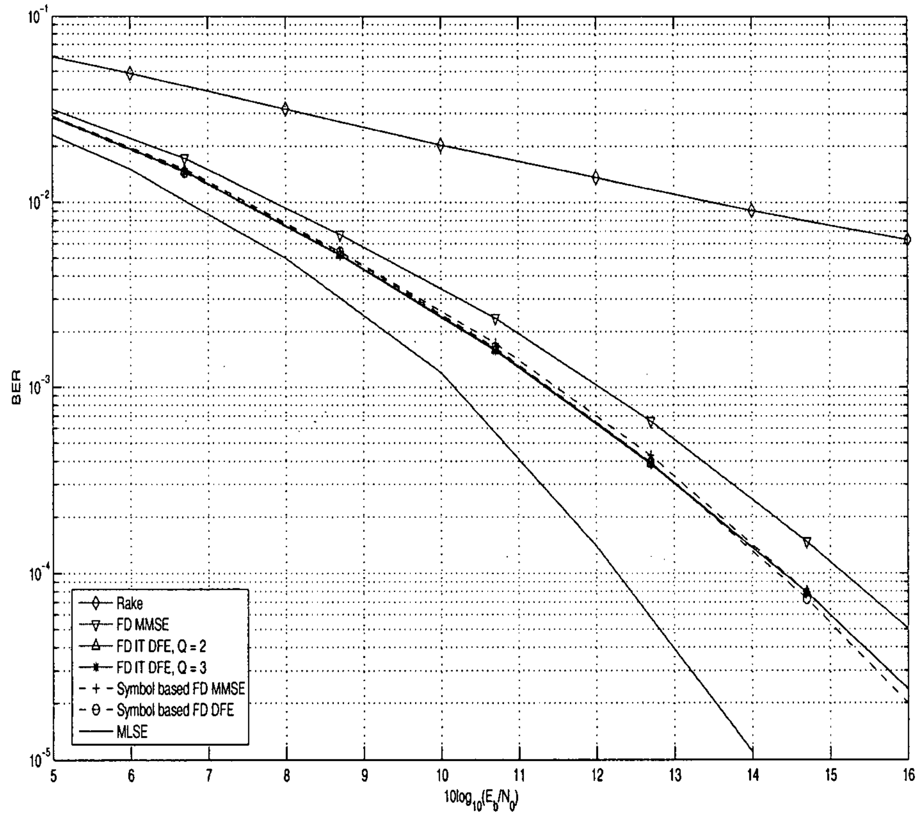

Figure 2.7: BER performance of various frequency domain equalizers for a BPSK DS-UWB system with spreading factor $N_s = 12$

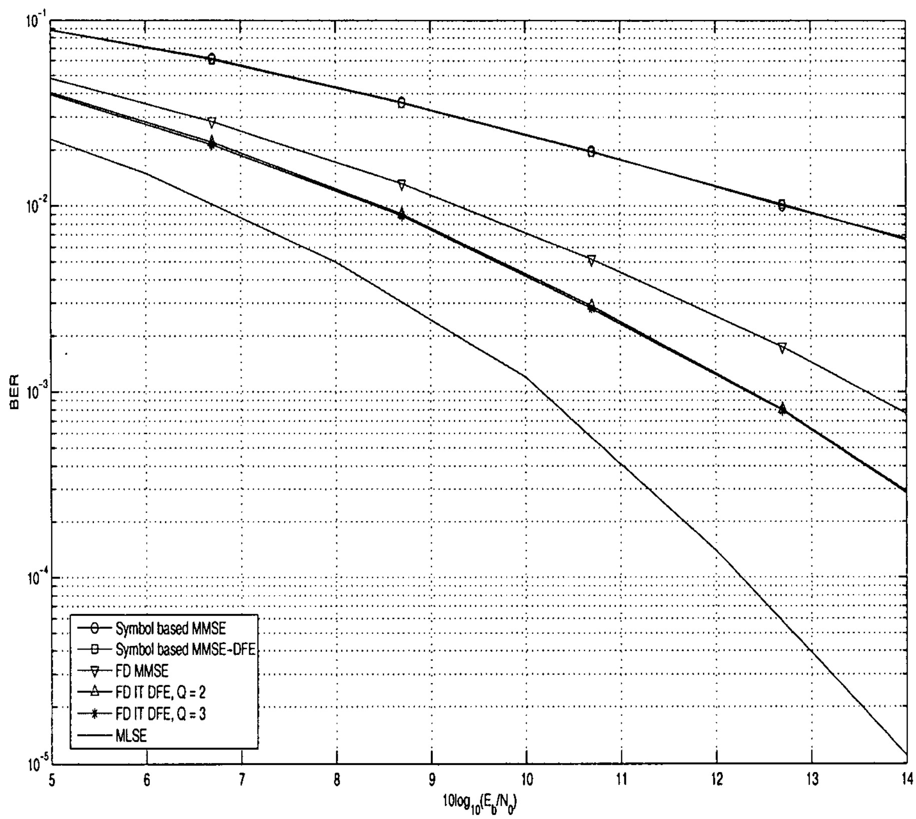

Figure 2.8: BER performance of frequency domain equalizers for a 4BOK DS-UWB system with spreading factor $N_s = 12$

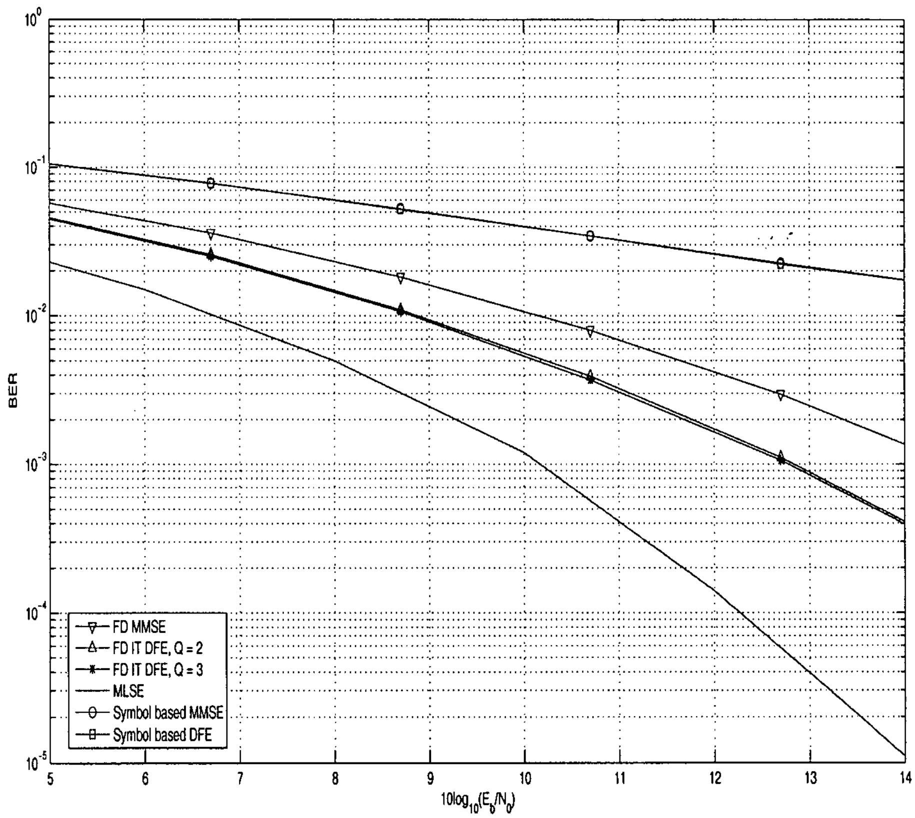

Figure 2.9: BER performance of frequency domain equalizers for a 4BOK DS-UWB system with spreading factor $N_s = 6$

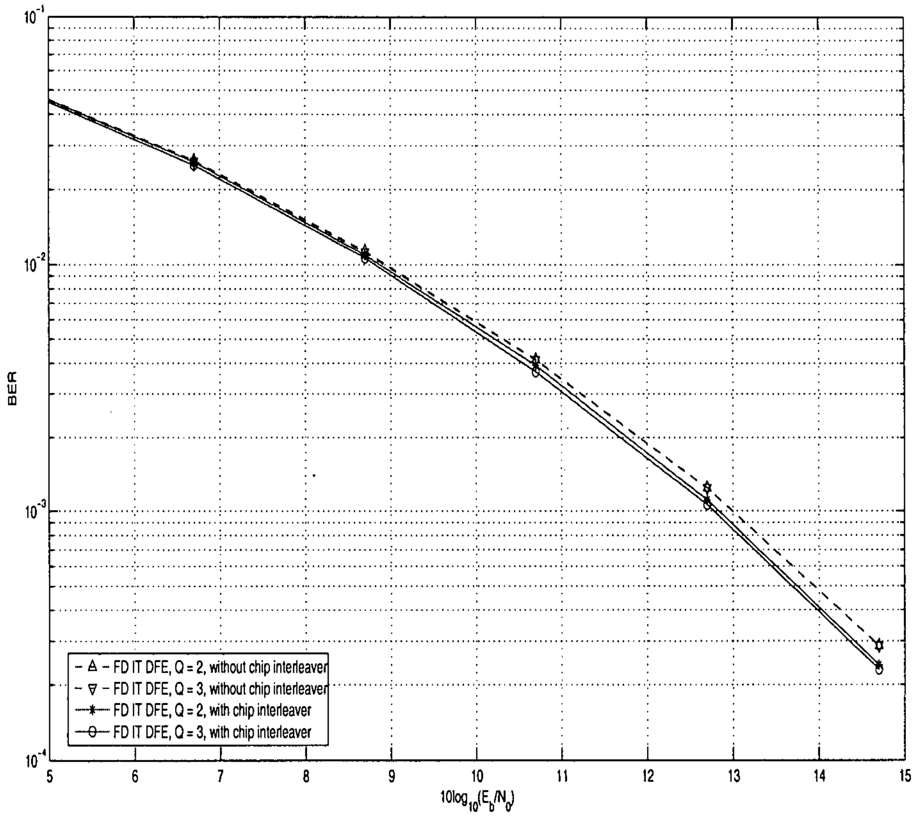

Figure 2.10: BER performance of FD IT DFE using chip interleaver and FD IT DFE without using chip interleaver for a 4BOK DS-UWB system with spreading factor $N_s = 6$

Table 2.4: Computational complexity of the receiver per output symbol for BPSK system with $N_s = 6$

Equalizer	No. of complex multi. per detected symbol
Rake	96
Rake MMSE	126 for $N_f = 30$ 146 for $N_f = 50$
Rake DFE	126 for $N_f = 30$ 146 for $N_f = 50$
FD MMSE	63.51
FD-IT-DFE	169.2 for $Q = 2$ 256.8 for $Q = 3$
symbol FD-MMSE	63.51
symbol FD-DFE	111.6

Table 2.5: Complexity of equalizer design per block for BPSK system with $N_s = 6$

Equalizer	Order of complexity
Rake MMSE	2500 for $N_f = 30$ 4900 for $N_f = 50$
Rake DFE	2500 for $N_f = 30$ 4900 for $N_f = 50$
FD MMSE	1536
FD-IT-DFE	3582 for $Q = 2$ 5373 for $Q = 3$
symbol FD MMSE	1536
symbol FD-DFE	10651

mance than chip based equalizers for BPSK DS-UWB systems. However, symbol based frequency domain equalizers do not perform well for 4BOK system compared to chip based equalization schemes.

Chapter 3

Multiuser Detection

3.1 Introduction

Performance of conventional rake receivers is severely degraded in the presence of multiple access interference (MAI). Multiuser detection schemes to eliminate MAI have been proposed for DS-UWB system in [19]. However, the complexity of these schemes can be quite high especially for long channels. In this chapter, we propose receiver structures for DS-UWB systems, in which multiuser detection and equalization are entirely performed in frequency domain, thus, significantly reducing the computational complexity.

Performance of the frequency domain MMSE linear multiuser receiver for DS-CDMA systems was investigated in [29]. Iterative frequency domain multiuser detection techniques have been proposed for BPSK and 4BOK DS-CDMA systems in [17]. In this Chapter, successive interference cancelation (SIC) and parallel interference cancelation (PIC) techniques are used to eliminate MAI in DS-UWB systems. Receiver structures employed are similar to those employed in [17]. We also consider single user 4BOK system as a two-user BPSK system and apply multiuser detection schemes.

3.2 System Model

A DS-UWB system with U users is considered. The multiuser system model is shown in Fig 3.1. $d_u[i], i = 0, 1, ..., M-1$ represents the u^{th} user data sequence. $s'_u[k], k = 0, 1, ..., MN_s - 1$ is the chip sequence obtained after spreading. $s_u[k], k = 0, 1, ..., N-1$ is obtained from $s'_u[k]$ by adding the pseudo random prefix of length L_p. A_u is the

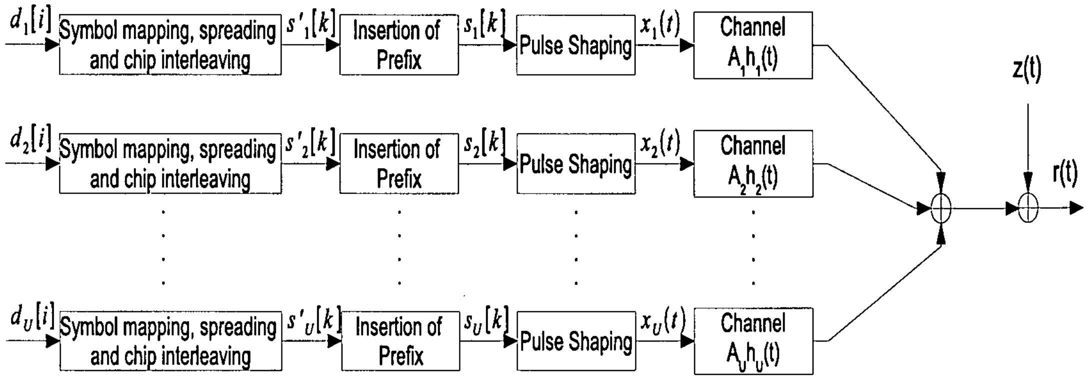

Figure 3.1: Transmitter and channel for a multiuser DS-UWB system

amplitude of the user u at the receiver. Users are indexed in decreasing order of power. Uplink of a synchronous DS-UWB system is considered. At the receiver, after pulse matched filtering, chip rate sampling, and taking the DFT, for each transmitted block we have

$$R(n) = \sum_{u=1}^{U} A_u H_u(n) S_u(n) + Z(n) \qquad n = 0, 1, ..., N-1 \tag{3.1}$$

where $S_u(n)$ and $H_u(n)$ are DFTs of $s_u[k]$ and $h_u[k]$ respectively.

3.3 Successive Interference Cancelation

The receiver structure employing SIC is shown in Fig 3.2. In SIC, interference cancelation is performed serially for each user. Users are detected in decreasing order of their power. Without loss of generality, here we assume that the users are indexed in decreasing order of their power. For the first user, the user bits of other users are unknown and are assumed to be independent and identically distributed. Equalizer structures from Section 2.4 are used to detect the user 1. After user 1 is detected, the interference caused due to user 1 on other users is removed, assuming that user 1 has been detected correctly. For second user, user bits $u = 3, ..., U$ are as unknown are assumed to be independent and identically distributed. This process is iteratively done till all the U are detected.

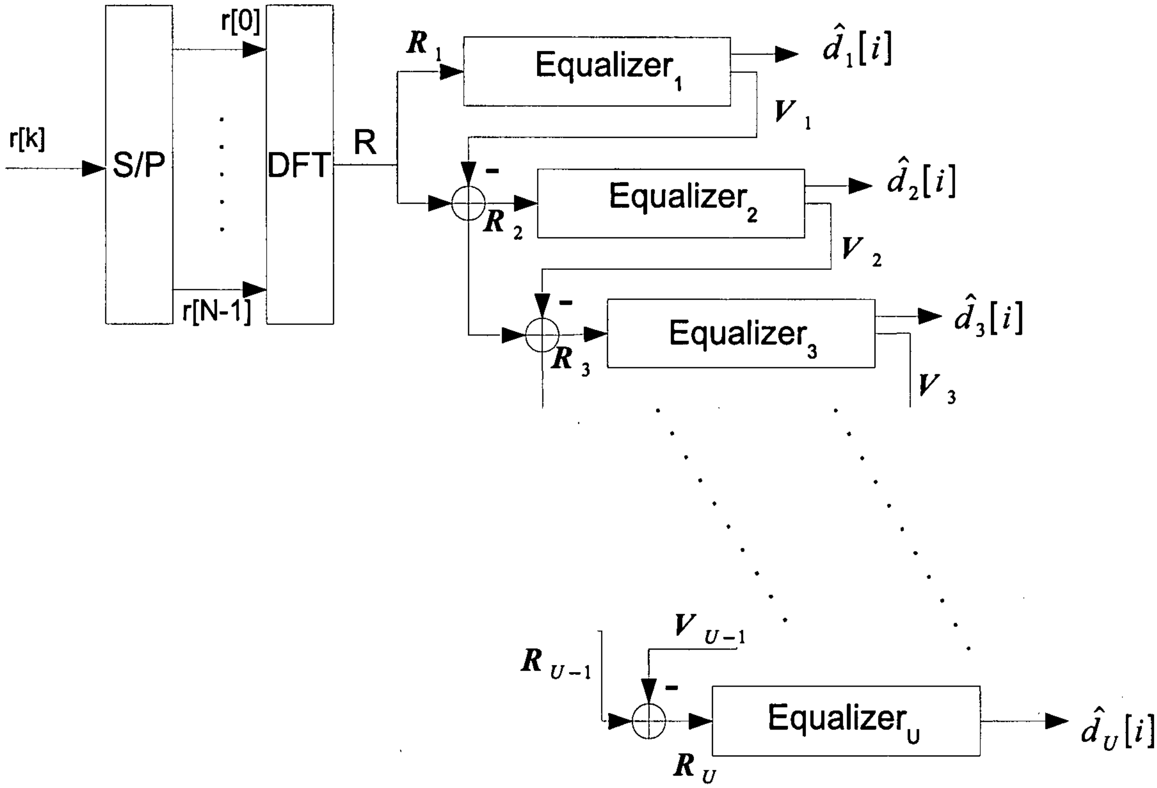

Figure 3.2: Successive interference cancelation

Either a frequency domain MMSE equalizer or iterative frequency domain decision feedback equalizer can be employed to detect each user. The frequency domain MMSE equalizer for user u is given by [17]

$$W_u(n) = \frac{H_u(n)^*}{N_s\sigma^2 + \sum_{u'=u}^{U} A_{u'}^2 |H_{u'}(n)|^2} \qquad n = 0, 1, ..., N-1 \tag{3.2}$$

For iterative decision feedback equalization, feedforward filter for u^{th} user and q^{th} iteration is given by

$$W_u^q(n) = \frac{H_u(n)^*}{N_s\sigma^2 + A_u^2\left(1 - |\rho_u^q|^2\right)|H_u(n)|^2 + \sum_{u'=u+1}^{U} A_{u'}^2 |H_{u'}(n)|^2} \tag{3.3}$$

where

$$\rho_u^q = \frac{\nu}{A_u E_u}\left(1 + \frac{\sigma^2 N_s}{A_u^2 X_u^2}\right)\sum_{n=0}^{N-1} \frac{R(n) H_u(n)^*}{\frac{A_u^2}{N_s}|H_u(n)|^2 + \sigma^2} \hat{S}_u^{q-1}(n)^* \tag{3.4}$$

where $E_u = E\left[\sum_{n=0}^{N-1} |S_u(n)|^2\right] = \frac{N^2}{N_s}$ and X_u represents the log normal shadowing factor of the channel impulse $h_u(t)$. The feedback filter at q^{th} iteration is given by

$$B_u^q(n) = -\rho_u^q\left[H_u(n) W_u^q(n) - \gamma_u^q\right] \tag{3.5}$$

where

$$\gamma_u^q = \frac{1}{N}\sum_{n=0}^{N-1} H_u(n) W_u^q(n) \tag{3.6}$$

3.4 Parallel Interference Cancelation

The receiver structure employing parallel interference cancelation is shown in Fig 3.3. In PIC, interference cancelation is performed in parallel for all users. During the first iteration, for each user, equalizers proposed in Section 2.4 is used to detect the user symbols treating that signals of all other users as unknown. Then the estimates of the symbols so obtained are used to cancel the interference of other users on each user. During 2nd iteration , equalizers detect each user assuming the residual interference from other users as Gaussian. This process is carried iteratively.

Let P be the number of iterations used for interference cancelation. MMSE equal-

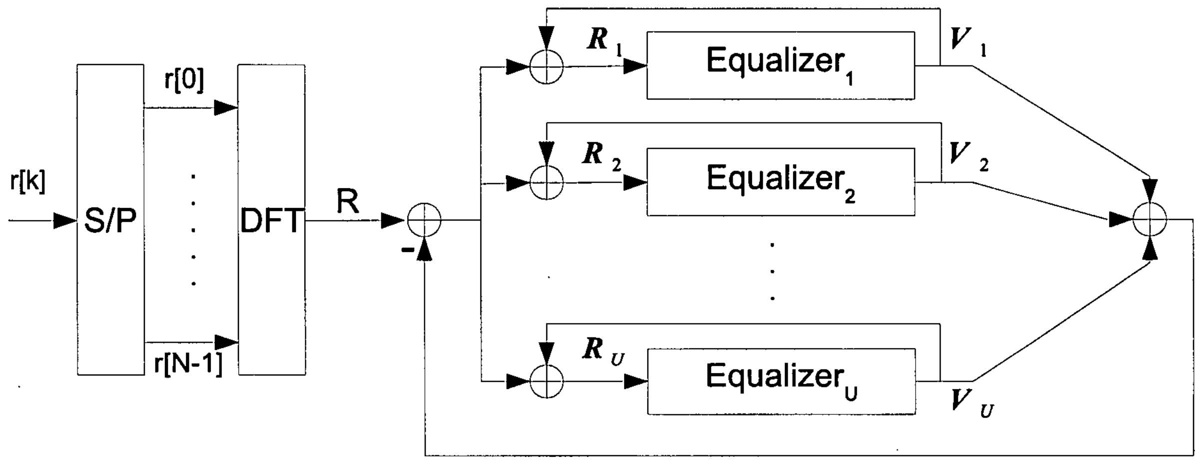

Figure 3.3: Parallel interference cancelation

izer for user u at p^{th} iteration is given by [17]

$$W_u^p(n) = \frac{H_u(n)^*}{N_s\sigma^2 + \sum_{u'=1}^{U}(1-|\hat{\rho}_{u'}^p|^2)\, A_{u'}^2 |H_{u'}(n)|^2} \qquad n = 0, 1, ..., N-1 \tag{3.7}$$

where

$$\hat{\rho}_u^p = \frac{\nu}{A_u E_u}(1 + \frac{\sigma^2 N_s}{A_u^2 X_u^2}) \sum_{n=0}^{N-1} \frac{R(n) H_u(n)^*}{\frac{A_u^2}{N_s}|H_u(n)|^2 + \sigma^2} \hat{S}_u^{p-1}(n)^* \tag{3.8}$$

where $\hat{S}_u^{p-1}(n)$ is the FFT of the chip sequence corresponding to estimates of u^{th} user bits after $p-1^{th}$ PIC iteration. For iterative decision feedback equalization, the feedforward filter at q^{th} iteration is given by [17]

$$W_u^{p,q}(n) = \frac{H_u(n)^*}{N_s\sigma^2 + A_u^2\,(1 - |\rho_u^{p,q}|^2)\,|H_u(n)|^2 + \sum_{u' \neq u} A_{u'}^2\,(1 - |\hat{\rho}_{u'}^p|^2)\,|H_{u'}(n)|^2} \tag{3.9}$$

where

$$\rho_u^{p,q} = \frac{\nu}{A_u E_u}(1 + \frac{\sigma^2 N_s}{A_u^2 X_u^2}) \sum_{n=0}^{N-1} \frac{R(n) H_u(n)^*}{\frac{A_u^2}{N_s}|H_u(n)|^2 + \sigma^2} \hat{S}_u^{p-1,q-1}(n)^* \tag{3.10}$$

$$\hat{\rho}_u^p = \rho_u^{p,Q} \tag{3.11}$$

where $E_u = \sum_{n=0}^{N-1} |S_u(n)|^2 = \frac{N^2}{N_s}$. $\hat{S}_u^{p-1,q-1}(n)$ is the FFT of the chip sequence corresponding to estimates of u^{th} user bits after $q-1^{th}$ equalizer iteration and $p-1^{th}$ PIC iteration. The feedback filter at q^{th} iteration is given by [17]

$$B_u^{p,q}(n) = -\rho_u^q \left[H_u(n)W_u^{p,q}(n) - \gamma_u^{p,q}\right] \tag{3.12}$$

where

$$\gamma_u^{p,q} = \frac{1}{N}\sum_{n=0}^{N-1} H_u(n)W_u^{p,q}(n) \tag{3.13}$$

3.5 Single user 4BOK system

As shown in Section 2.5.2, single user 4BOK system can be treated as a 2 user BPSK system. So, above multiuser detection schemes (PIC and SIC) can be applied for a single user BPSK system. We apply these schemes for single user 4BOK system and compare their performance with equalization schemes proposed in chapter 2.

3.6 Simulation results

We consider 4-user BPSK DS-UWB systems using ternary spreading sequences of length $N_s = 12$. All users are assumed to have equal transmit power. We simulate the average BER performance for CM4 channel model [22]. We consider transmission in lower band (3.1-4.85 GHz). We assume complete channel information at the receiver.

The ternary spreading codes of the 4 users are given by

Table 3.1: Ternary codes used for the 4 users

$\frac{1}{\sqrt{(11)}}[0\ -1\ -1\ -1\ 1\ 1\ 1\ -1\ 1\ 1\ -1\ 1]$
$\frac{1}{\sqrt{(11)}}[-1\ 1\ -1\ -1\ 1\ -1\ -1\ -1\ 1\ 1\ 1\ 0]$
$\frac{1}{\sqrt{(11)}}[0\ -1\ 1\ -1\ -1\ 1\ -1\ -1\ -1\ 1\ 1\ 1]$
$\frac{1}{\sqrt{(11)}}[-1\ -1\ -1\ 1\ 1\ 1\ -1\ 1\ 1\ -1\ 1\ 0]$

The decision feedback correction factor ν is chosen to be 0.8. Fig 3.4 shows the average BER performance of receiver using SIC for number of equalization iterations, $Q = 1, 2, 3$. Fig 3.5 shows the average BER performance of receiver using PIC for number of PIC iterations $P = 1, 2, 3$ and number of equalization iterations $Q = 1, 2$.

It can be seen from the simulation results that significant improvement in the performance is achieved during first two PIC and first two equalization iterations.

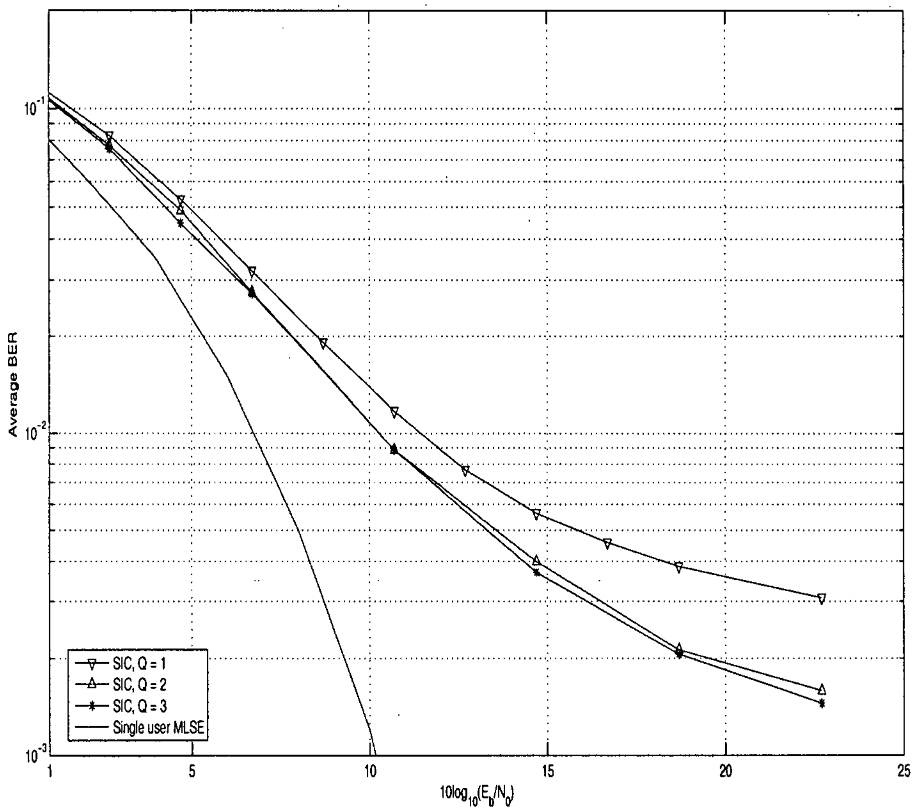

Figure 3.4: BER performance of receiver employing successive interference cancelation for a 4-user BPSK DS-UWB system with spreading factor $N_s = 12$

The improvement in performance with further equalization or interference cancelation iterations is not so significant.

For single user 4BOK case, performance improvement is observed over the symbol based 4BOK system but it is not as good as the chip based equalizers.

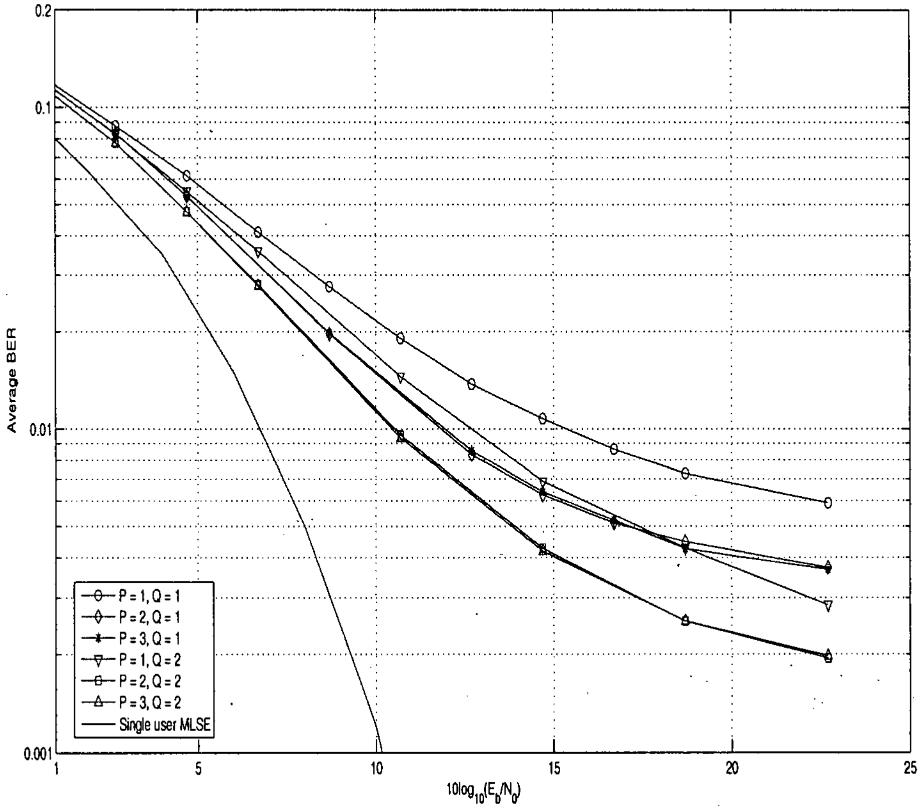

Figure 3.5: BER performance of receiver employing parallel interference cancelation for a 4-user BPSK DS-UWB system with spreading factor $N_s = 12$

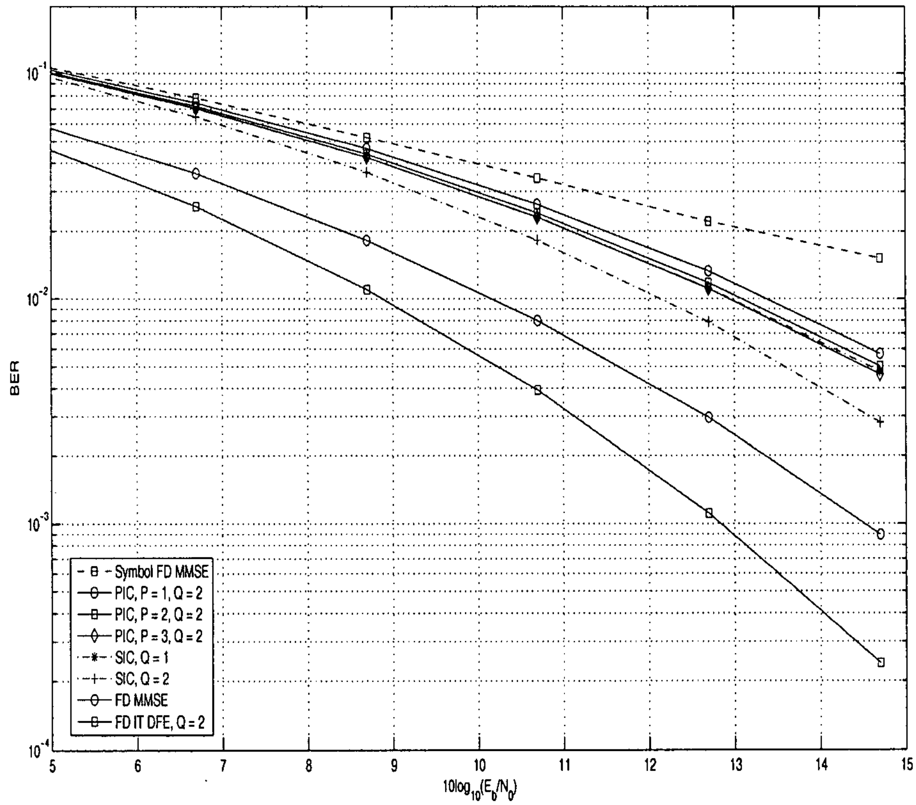

Figure 3.6: BER performance of receiver employing multiuser detection techniques for a single user 4BOK DS-UWB system with spreading factor $N_s = 6$

Chapter 4

Turbo Equalization

4.1 Introduction

In this chapter, we consider a DS-UWB system with a forward error correction(FEC) scheme. Usually for the coded systems, decoding and equalization are carried out separately at the receiver. An equalizer is used to compensate for channel effects and make estimate of channel transmitted symbols. From these symbol estimates, a de-mapper is used to obtain estimates of interleaved coded bits. Then a de-interleaver and a decoder are used to obtain the information bits.

However, the above process of making hard decisions by the equalizer destroys the information regarding how likely each code bit might have been. There are many decoders which exploit this "soft" information to give a better performance. In turn, the decoder can generate its own soft information and this soft information can be exploited at the equalizer to improve channel symbol estimates. This process can be carried on iteratively.

When processing soft information regarding a given bit, it is assumed that the soft information about each bit is independent. This assumption enables use of simple and fast algorithms for equalizer and decoder. However, this assumption can only be valid if the soft information of a given bit is generated based on soft information of bits other than the given bit. This information is called the "extrinsic information". The process of passing extrinsic information recursively between equalizer and decoder is essential for turbo decoding [30]. The extrinsic information is expressed by log likelihood ratios(LLRs).

The equalizer used could either be trellis based, linear or decision feedback. However, trellis based equalizers generally have very high complexity. So linear or decision

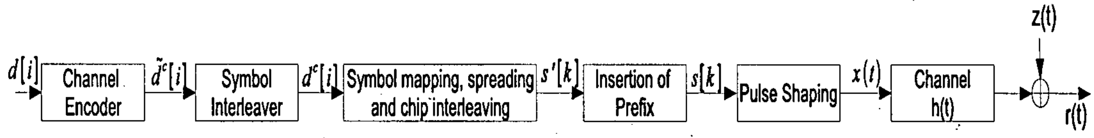

Figure 4.1: Transmitter and channel for single user coded DS-UWB system

feedback equalizers are used. Turbo equalization schemes with MMSE equalization in time domain have been studied in [31]. In [28], a turbo equalization scheme in which MMSE equalization is carried in frequency domain was proposed for BPSK SC systems.

In this chapter, we propose low complexity frequency domain MMSE turbo equalization schemes for single user BPSK and 4BOK DS-UWB systems based on the frequency domain turbo equalization scheme proposed for single carrier BPSK systems in [32]. We later consider multiuser DS-UWB system. We combine the single user frequency domain turbo equalization schemes with soft interference cancelation [34] to obtain multiuser frequency domain turbo detectors. The multiuser turbo detector is then applied over single user 4BOK system by considering it as a two-user BPSK system. Maximum *a* posteriori (MAP) decoder is used in all the schemes. Cyclic prefix is used for all the systems presented in this chapter.

4.2 Single User System

The transmitter structure for a single user DS-UWB system is shown in Fig 4.1. The receiver structure is shown in Fig 4.2.

4.2.1 BPSK System

First, a single user BPSK DS-UWB system is considered.

Let $L_c(d^c) = [L_c(d^c[0]), L_c(d^c[1]), L_c(d^c[2]), ..., L_c(d^c[M-1])]$ represent the log likelihood ratios of the symbols obtained from the decoder and interleaver. The log likelihood ratio is defined as

$$L_c(d^c) = \log \frac{p(d^c = 1)}{p(d^c = -1)} \tag{4.1}$$

The structure of the frequency domain SISO equalizer is shown in Fig 4.3. Soft

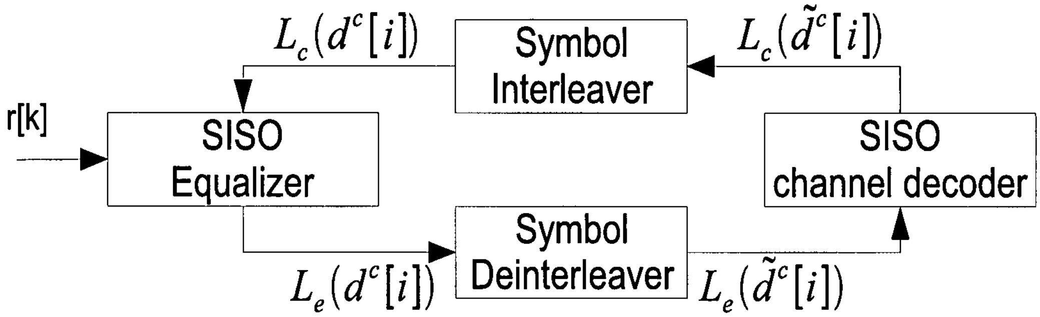

Figure 4.2: Receiver for single user coded DS-UWB system

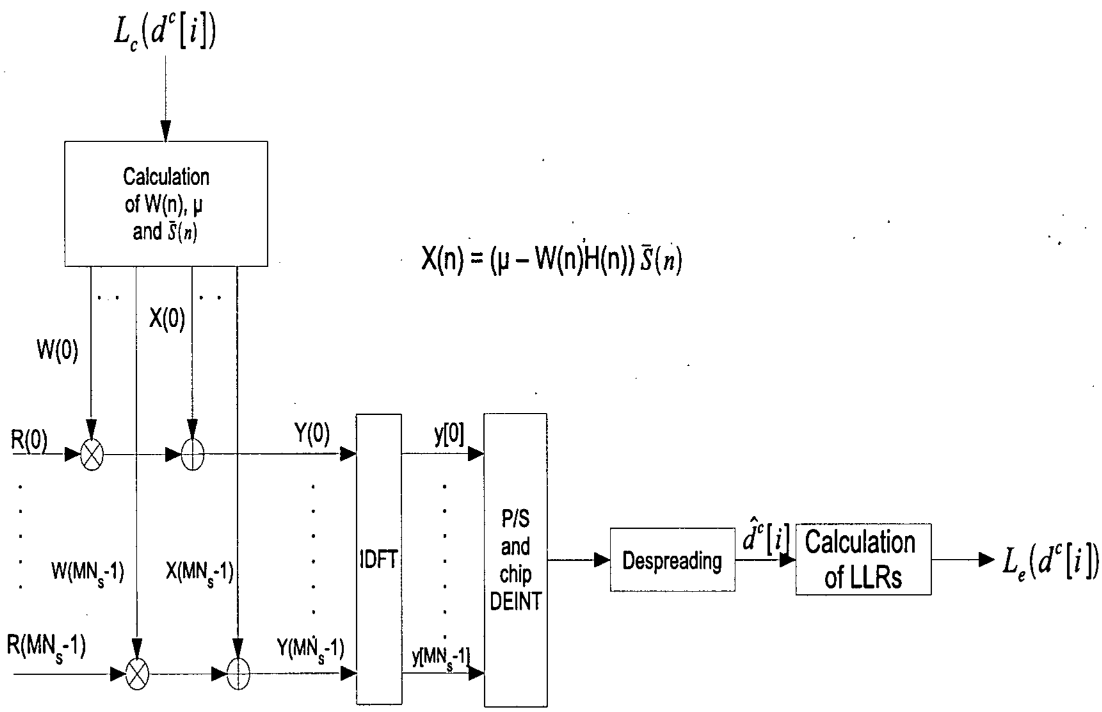

Figure 4.3: Frequency domain SISO equalizer for single user coded MBOK DS-UWB system

bit estimates $\bar{d}^c[i]$ are first obtained using the *a* priori information from the channel decoder.

$$\bar{d}^c[i] = \tanh(0.5L_c(d^c[i])) \tag{4.2}$$

After spreading and addition of prefix, soft chip sequence estimate $\bar{s}[k]$ is obtained. The FFT of $\bar{s}[k]$ is represented by $\bar{S}(n)$. Frequency domain chip sequence $\{S(n)\}_{n=0}^{n=MN_s-1}$ is assumed to be independent and identically distributed with mean zero and variance σ_S^2. This assumption makes the turbo equalization schemes proposed in this chapter suboptimal. However, this greatly reduces the computational complexity of the equalizer. Now, the average energy of chip sample for time domain signal $s[k]$ is $E(|s[k]|^2) = \frac{1}{N_s}$ (as energy per symbol is chosen as 1), $E(|S(n)|^2) = MN_sE(|s[k]|^2) = M$. Since mean of $S(n)$ is zero, $\sigma_S^2 = E(|S(n)|^2) = M$.

Using statistical estimation theory, it has been shown in [32] that $\bar{S}(n)$ can be modeled as a zero mean and uncorrelated sequence with variance $\sigma_{\bar{S}}^2 \approx \frac{1}{MN_s}\sum_{n=0}^{MN_s-1}|\bar{S}(n)|^2$. $\bar{S}(n)$ and $\sigma_{\bar{S}}^2$ are required for the frequency domain soft MMSE equalization.

A MMSE SISO equalizer minimizes the metric

$$\begin{aligned} J &= E\left[|y[k] - s[k]|^2\right] \\ &= \frac{1}{(MN_s)^2}\sum_{n=0}^{MN_s-1} E\left[|Y(n) - S(n)|^2\right] \\ &= \frac{1}{(MN_s)^2}\sum_{n=0}^{MN_s-1} E\left[|W(n)R(n) + B(n)\bar{S}(n) - S(n)|^2\right] \end{aligned} \tag{4.3}$$

subject to constraint

$$\frac{1}{MN_s}\sum_{n=0}^{MN_s-1} B(n) = 0 \tag{4.4}$$

To minimize J, its sufficient to minimize

$$J(n) = E\left[|W(n)R(n) + B(n)\bar{S}(n) - S(n)|^2\right] \tag{4.5}$$

for all $n = 0, 1, ..., MN_s - 1$.

The cost function to be minimized for each n, is given by

$$J_\beta(n) = E\left[|W(n)R(n) + B(n)\bar{S}(n) - S(n)|^2\right] + \beta\left(\frac{1}{MN_s}\sum_{n=0}^{MN_s-1} B(n)\right) \tag{4.6}$$

where β is the Lagrange multiplier to account for the constraint.

Minimizing the above cost function, we arrive at following equalization algorithm (see Appendix B):

$$\bar{S} = FFT(\bar{s}) \tag{4.7}$$

$$\sigma_{\bar{S}}^2 = \frac{1}{MN_s}\sum_{n=0}^{MN_s-1}|\bar{S}(n)|^2 \tag{4.8}$$

$$\tilde{W}(n) = \frac{H(n)^*}{MN_s\sigma^2 + (\sigma_S^2 - \sigma_{\bar{S}}^2)|H(n)|^2} \tag{4.9}$$

$$\tilde{\mu} = \frac{1}{MN_s}\sum_{n=0}^{MN_s-1}\tilde{W}(n)H(n) \tag{4.10}$$

$$\lambda = \frac{\sigma_S^2}{1+\sigma_{\bar{S}}^2\tilde{\mu}} \tag{4.11}$$

$$W(n) = \lambda\tilde{W}(n) \tag{4.12}$$

$$\mu = \lambda\tilde{\mu} \tag{4.13}$$

$$Y(n) = W(n)R(n) + (\mu - W(n)H(n))\bar{S}(n) \tag{4.14}$$

Output after soft MMSE filtering can be assumed to be an output of an equivalent AWGN channel with input $s[k]$ [34].

$$\begin{aligned} y[k] &= \mu s[k] + z[k] \\ &= \mu d^c\left[\lfloor\frac{k}{N_s}\rfloor\right] c\left[k - \lfloor\frac{k}{N_s}\rfloor\right] + z[k] \end{aligned} \tag{4.15}$$

It can be shown that for MMSE filtering (see Appendix B)

$$\begin{aligned} E(|y[k]-s[k]|^2) &= \frac{1}{MN_s}\sigma_S^2(1-\mu) \\ &= \frac{1}{N_s}(1-\mu) \end{aligned} \tag{4.16}$$

Variance of $z[k], \sigma_z^2$ can be found from above as follows

$$\begin{aligned}
\frac{1}{N_s}(1-\mu) &= E(|y[k]-s[k]|^2) \\
&= E(|(\mu-1)s[k]+z[k]|^2) \\
&= (1-\mu)^2\frac{1}{N_s}+\sigma_z^2 \\
\Longrightarrow \sigma_z^2 &= \frac{1}{N_s}\mu(1-\mu) \qquad (4.17)
\end{aligned}$$

LLRs generated by the equalizer are given by

$$\begin{aligned}
L_e(d^c[i]) &= \log\frac{p(\{y[k]\}_{k=(i-1)N_s}^{k=iN_s-1}|d^c[i]=1)}{p(\{y[k]\}_{k=(i-1)N_s}^{k=iN_s-1}|d^c[i]=-1)} \\
&= \sum_{j=0}^{N_s-1} -\frac{(y[(i-1)N_s+j]-\mu c[j])^2}{2\frac{1}{N_s}\mu(1-\mu)} + \frac{(y[(i-1)N_s+j]+\mu c[j])^2}{2\frac{1}{N_s}\mu(1-\mu)} \\
&= \frac{2N_s\sum_{j=0}^{N_s-1} y[(i-1)N_s+j]c[j]}{1-\mu} \\
&= \frac{2N_s\hat{d}^c[i]}{1-\mu} \quad \text{where} \quad \hat{d}^c[i] = \sum_{j=0}^{N_s-1} y[(i-1)N_s+j]c[j] \qquad (4.18)
\end{aligned}$$

It should be noted that a single MMSE frequency domain filter is used for all bits in a transmitted block unlike time domain turbo equalization in which different filter coefficients are used for each bit. Although this degrades the performance of the turbo equalizer, it significantly reduces the computational complexity.

4.2.2 4BOK System

LLRs of the bits generated by the decoder are given by
$L_c(d^c) = [L_c(d^c[0]), L_c(d^c[1]), L_c(d^c[2]), ..., L_c(d^c[2M-1])]$.

The structure of the frequency domain SISO equalizer is shown in Fig 4.3. Soft bit estimates $\bar{d}^c[i]$ are first obtained using the *a* priori information from the channel decoder.

$$\bar{d}^c[i] = \tanh(0.5L_c(d^c[i])) \qquad (4.19)$$

After spreading and addition of prefix, soft chip sequence estimate $\bar{s}[k]$ is obtained. Frequency domain chip sequence $\{S(n)\}_{n=0}^{n=MN_s-1}$ is assumed to be independent and identically distributed with mean zero and variance $\sigma_S^2 = M$. Now the LLRs of the bits $d^c[i]$ are obtained in a way very similar to that of BPSK. First equalization is performed using equation (4.7-4.14) to obtain $Y(n)$. Inverse FFT is performed over $Y(n)$ to obtain $y[k]$.

Output after soft MMSE filtering can be assumed to be an output of an equivalent AWGN channel with input $s[k]$.

$$\begin{aligned} y[k] &= \mu s[k] + z[k] \\ &= \mu\{\tilde{s}_1[k] + \tilde{s}_2[k]\} + z[k] \\ &= \mu d^c\left[2\lfloor\frac{k}{N_s}\rfloor\right]\tilde{c}_1\left[k - \lfloor\frac{k}{N_s}\rfloor\right] + \mu d^c\left[2\lfloor\frac{k}{N_s}\rfloor + 1\right]\tilde{c}_2\left[k - \lfloor\frac{k}{N_s}\rfloor\right] + z[k] \end{aligned} \tag{4.20}$$

As shown in Section 2.5.2, 4BOK user can be seen as a 2-user BPSK system. Therefore, at the receiver, after matched filtering and chip rate sampling, we have

$$r[k] = \sum_{l=0}^{L_s-1} h[l]s[k-l] + z[k] = \sum_{l=0}^{L_s-1} h[l]\{\tilde{s}_1[k-l] + \tilde{s}_2[k-l]\} + z[k] \qquad k = 0, 1, ..., MN_s + L_p - 1 \tag{4.21}$$

where $\tilde{s}_1$ and $\tilde{s}_2$ are obtained from $\tilde{s}'_1$ and $\tilde{s}'_2$ respectively by adding corresponding cyclic prefixes.

For calculating the LLRs of $d^c[2i]$, $\tilde{s}_2[k]$ is assumed to be zero mean Gaussian distributed and independent of $\tilde{s}_1[k]$. Similar to the case of BPSK, variance of the interference $z[k] + \mu\tilde{s}_2[k], \sigma^2_{inter}$ can be obtained as follows

$$\begin{aligned} \frac{1}{N_s}(1-\mu) &= E(|y[k] - s[k]|^2) \\ &= E(|(\mu - 1)\tilde{s}_1[k] + z[k] + \mu\tilde{s}_2[k]|^2) \\ &= (1-\mu)^2\frac{1}{2N_s} + \sigma^2_{inter} \\ \Longrightarrow \sigma^2_{inter} &= \frac{1}{2N_s}(1-\mu^2) \end{aligned} \tag{4.22}$$

$$
\begin{aligned}
L_e(d^c[2i]) &= \log \frac{p(\{y[k]\}_{k=(i-1)N_s}^{k=iN_s-1}|b[i]=1)}{p(\{y[k]\}_{k=(i-1)N_s}^{k=iN_s-1}|b[i]=-1)} \\
&= \sum_{j=0}^{N_s-1} -\frac{(y[(i-1)N_s+j] - \mu\tilde{c}_1[j])^2}{2\frac{1}{2N_s}(1-\mu^2)} + \frac{(y[(i-1)N_s+j] + \mu\tilde{c}_1[j])^2}{2\frac{1}{2N_s}(1-\mu^2)} \\
&= \frac{4N_s\mu\sum_{j=0}^{N_s-1} y[(i-1)N_s+j]\tilde{c}_1[j]}{1-\mu^2} \\
&= \frac{4N_s\mu\hat{d}^c[2i]}{1-\mu^2} \quad \text{where} \quad \hat{d}^c[2i] = \sum_{j=0}^{N_s-1} y[(i-1)N_s+j]\tilde{c}_1[j] \qquad (4.23)
\end{aligned}
$$

Similarly, LLRs of $d^c[2i+1]$ can be obtained as

$$
\begin{aligned}
L_e(d^c[2i+1]) &= \frac{4N_s\mu\sum_{j=0}^{N_s-1} y[(i-1)N_s+j]\tilde{c}_2[j]}{1-\mu^2} \\
&= \frac{4N_s\mu\hat{d}^c[2i+1]}{1-\mu^2} \quad \text{where} \quad \hat{d}^c[2i] = \sum_{j=0}^{N_s-1} y[(i-1)N_s+j]\tilde{c}_2[j]
\end{aligned}
\qquad (4.24)
$$

4.3 Multiuser System

In this section, U user DS-UWB system is considered. Soft interference cancelation [34] is used to mitigate MAI and soft MMSE filter is used to tackle ISI. The transmitter and receiver structure for multiuser DS-UWB systems are shown in Fig 4.4 and Fig 4.5, respectively.

First, soft estimates of bits of all users are obtained based on *a* priori information from the U decoders.

$$\bar{d}_u^c[i] = \tanh(0.5L_e(d_u^c[i])) \qquad (4.25)$$

After spreading and prefix addition for each user u, soft chip sequence estimate $\bar{s}_u[k]$ are obtained. Soft interference cancelation is then performed to eliminate the interference of all other users over the signal of a given user to obtain

$$R_u(n) = R(n) - \sum_{u' \neq u} A_{u'} H_{u'}(n) \bar{S}_{u'}(n) \qquad (4.26)$$

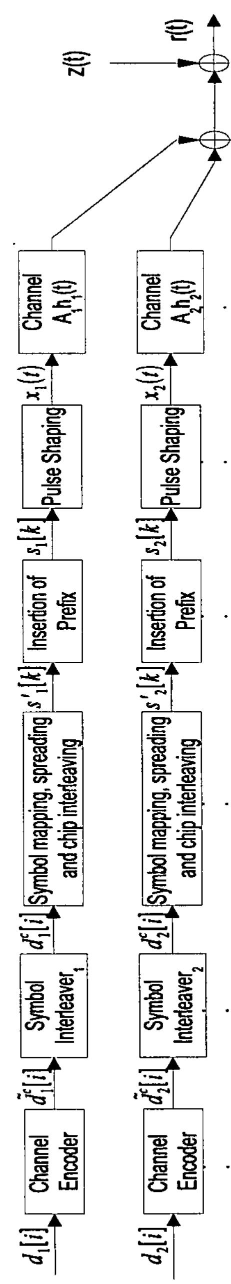

Figure 4.4: System model for multiuser coded DS-UWB system

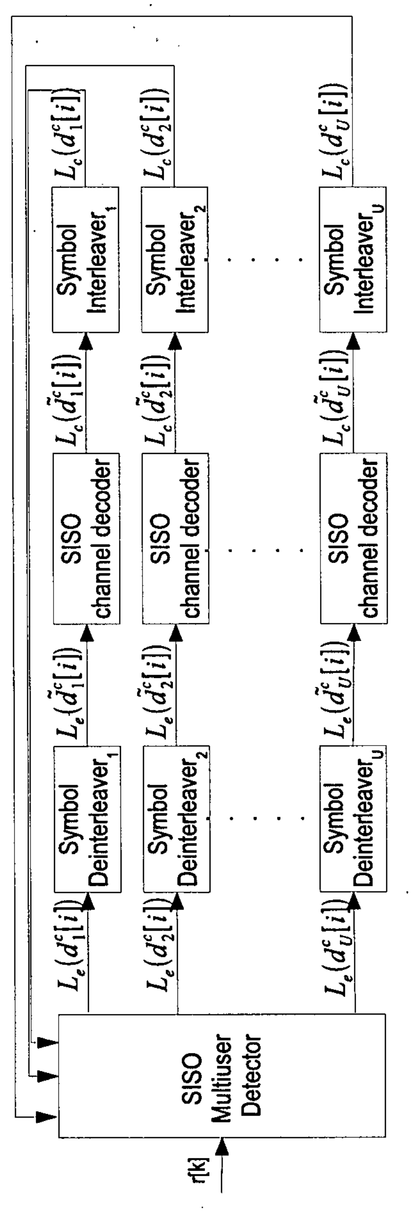

Figure 4.5: Receiver for multiuser coded DS-UWB system.

where $\bar{S}_u$ denotes FFT of $\bar{s}_u$. Similar to the single user case, $S_u(n)$ is assumed to be independent and identically distributed with zero mean and variance $\sigma^2_{S_u} = M$. Following equalization algorithm is used for each user

$$
\begin{aligned}
\sigma^2_{\bar{S}_u} &= \frac{1}{MN_s} \sum_{n=0}^{MN_s-1} |\bar{S}_u(n)|^2 && (4.27)\\
\tilde{W}_u(n) &= \frac{A_u^* H_u(n)^*}{MN_s\sigma^2 + \sum_{u'=1}^{U}(\sigma^2_{S_{u'}} - \sigma^2_{\bar{S}_{u'}})|A_{u'}H_{u'}(n)|^2} && (4.28)\\
\tilde{\mu}_u &= \frac{1}{MN_s} \sum_{n=0}^{MN_s-1} \tilde{W}_u(n) A_u H_u(n) && (4.29)\\
\lambda_u &= \frac{\sigma^2_{S_u}}{1+\sigma^2_{\bar{S}_u}\tilde{\mu}_u} && (4.30)\\
W_u(n) &= \lambda_u \tilde{W}_u(n) && (4.31)\\
\mu_u &= \lambda_u \tilde{\mu}_u && (4.32)\\
Y_u(n) &= W_u(n)R_u(n) + (\mu - W_u(n)A_uH_u(n))\bar{S}_u(n) && (4.33)
\end{aligned}
$$

For BPSK system, the spreading sequence of user u is denoted by $\{c[j;u]\}_{j=0}^{N_s-1}$. The LLRs for BPSK system are given by

$$
\begin{aligned}
L_e(d_u^c[i]) &= \frac{2N_s \sum_{j=0}^{N_s-1} y_u[(i-1)N_s + j]c[j;u]}{1-\mu_u}\\
&= \frac{2N_s \hat{d}_u^c[i]}{1-\mu_u} \quad \text{where} \quad \hat{d}_u^c[i] = \sum_{j=0}^{N_s-1} y_u[(i-1)N_s + j]c[j;u]
\end{aligned}
\qquad (4.34)
$$

For 4BOK system, the orthogonal spreading sequences of user u is denoted by

$\{c_1[j;u]\}_{j=0}^{N_s-1}$ and $\{c_2[j;u]\}_{j=0}^{N_s-1}$. The LLRs for 4BOK system are given by

$$\begin{aligned} L_e(d^c[2i]) &= \frac{4N_s\mu_u \sum_{j=0}^{N_s-1} y[(i-1)N_s+j]\tilde{c}_1[j;u]}{1-\mu_u^2} \\ &= \frac{4N_s\mu_u \hat{d}^c[2i]}{1-\mu_u^2} \quad \text{where} \quad \hat{d}^c[2i] = \sum_{j=0}^{N_s-1} y_u[(i-1)N_s+j]\tilde{c}_1[j;u] \quad (4.35) \\ L_e(d^c[2i+1]) &= \frac{4N_s\mu_u \sum_{j=0}^{N_s-1} y[(i-1)N_s+j]\tilde{c}_2[j;u]}{1-\mu_u^2} \\ &= \frac{4N_s\mu_u \hat{d}^c[2i+1]}{1-\mu_u^2} \quad \text{where} \quad \hat{d}^c[2i+1] = \sum_{j=0}^{N_s-1} y_u[(i-1)N_s+j]\tilde{c}_2[j;u] \\ & \qquad\qquad (4.36) \end{aligned}$$

with $\tilde{c}_1[j;u] = -\frac{c_1[j;u]+c_2[j;u]}{2}$ and $\tilde{c}_2[j;u] = \frac{-c_1[j;u]+c_2[j;u]}{2}$

4.3.1 Single user 4BOK system

As shown in Section 2.5.2, a single user 4BOK system is equivalent a two-user BPSK system. So, multiuser BPSK turbo equalization algorithm can be used for detection of information bits. First, soft estimates of the bits are obtained.

$$\bar{d}^c[i] = \tanh(0.5L_e(d^c[i])) \tag{4.37}$$

Spreading estimated user bits $\bar{d}^c[2i]$ with the spreading sequence $\tilde{c}_1$ and adding corresponding cyclic prefix, chip sequence $\bar{s}_1[k]$ is obtained. Similarly, from estimated user bits $\bar{d}^c[2i+1]$, chip sequence $\bar{s}_2[k]$ is obtained.

For user bits $d^c[2i]$, soft interference cancelation is performed to remove the interference from bits $d^c[2i+1]$

$$R_1(n) = R(n) - H(n)\bar{S}_2(n) \tag{4.38}$$

Similarly, for user bits $d^c[2i+1]$, we have

$$R_2(n) = R(n) - H(n)\bar{S}_1(n) \tag{4.39}$$

$\bar{S}_1$ and $\bar{S}_2$ represent FFTs of $\bar{s}_1$ and $\bar{s}_2$ respectively.

$\tilde{S}_1[k]$ and $\tilde{S}_2[k]$ are assumed to be independent and identically distributed with zero mean and variance $\sigma^2_{\tilde{S}_1} = \sigma^2_{\tilde{S}_2} = E(|\tilde{S}_2(n)|^2) = MN_sE(|\tilde{s}_2[k]|^2) = MN_s\frac{1}{2N_S} =$

$M/2$

For u = 1,2

$$\begin{aligned}
\sigma^2_{\bar{S}_u} &= \frac{1}{MN_s}\sum_{n=0}^{MN_s-1}|\bar{S}_u(n)|^2 && (4.40)\\
\tilde{W}_u(n) &= \frac{H_u(n)^*}{MN_s\sigma^2+\sum_{u'=1}^{U}(\sigma^2_{\tilde{S}_{u'}}-\sigma^2_{\bar{S}_{u'}})|H_{u'}(n)|^2} && (4.41)\\
\tilde{\mu}_u &= \frac{1}{MN_s}\sum_{n=0}^{MN_s-1}\tilde{W}_u(n)H_u(n) && (4.42)\\
\lambda_u &= \frac{\sigma^2_{\tilde{S}_u}}{1+\sigma^2_{\bar{S}_u}\tilde{\mu}_u} && (4.43)\\
W_u(n) &= \lambda_u\tilde{W}_u(n) && (4.44)\\
\mu_u &= \lambda_u\tilde{\mu}_u && (4.45)\\
Y_u(n) &= W_u(n)R_u(n)+(\mu-W_u(n)H_u(n))\bar{S}_u(n) && (4.46)
\end{aligned}$$

LLRs are given by

$$\begin{aligned}
L_e(d^c[2i]) &= \frac{4N_s\sum_{j=0}^{N_s-1}y_1[(i-1)N_s+j]\tilde{c}_1[j]}{1-\mu_1}\\
&= \frac{4N_s\hat{d}^c[2i]}{1-\mu_1} \quad \text{where} \quad \hat{d}^c[2i]=\sum_{j=0}^{N_s-1}y_1[(i-1)N_s+j]\tilde{c}_1[j] && (4.47)\\
L_e(d^c[2i+1]) &= \frac{4N_s\sum_{j=0}^{N_s-1}y_2[(i-1)N_s+j]\tilde{c}_2[j]}{1-\mu_2}\\
&= \frac{4N_s\hat{d}^c[2i+1]}{1-\mu_2} \quad \text{where} \quad \hat{d}^c[2i+1]=\sum_{j=0}^{N_s-1}y_2[(i-1)N_s+j]\tilde{c}_2[j]\\
& && (4.48)
\end{aligned}$$

This method has higher complexity since two forward equalization filters need to be evaluated for each block.

4.4 Simulation Results

A half-rate convolutional code with constraint length $\kappa = 6$ and generating polynomial $(65, 57)$ (notation in octal) is used [5]. The simulation parameters for single user as well as multiuser BPSK and 4BOK systems are same as those used in previous chapters. Transmission in lower band (3.1-4.85 GHz) over CM4 channel is considered.

Fig 4.6 and Fig 4.7 show the BER performance of turbo equalizers for coded BPSK DS-UWB systems with spreading factor $N_s = 6$ and $N_s = 12$ respectively. The performance of turbo equalizer with perfect *a* priori information is also shown. Fig 4.8 shows the performance of turbo equalizers for coded 4BOK DS-UWB systems with spreading factor$N_s = 6$. Fig 4.9 shows the average BER performance of turbo equalizers for 4-user BPSK DS-UWB system with spreading factor $N_s = 12$.

The performance gain of second turbo iteration over the first iteration is more significant compared to the performance gain of third iteration over the second iteration. The improvement in performance with each turbo iteration is higher for systems with spreading factor 6 than system with spreading factor 12. This is expected since the systems with lower spreading factor suffer from more severe ISI and hence exhibits much better performance after soft ISI cancelation. Performance gain is very high especially for multiuser systems.

Also from Fig 4.10, we can see that turbo equalization scheme proposed in Section 4.3.1 for single user 4BOK system gives better performance than the scheme proposed in Section 4.2.2 at the expense of higher complexity.

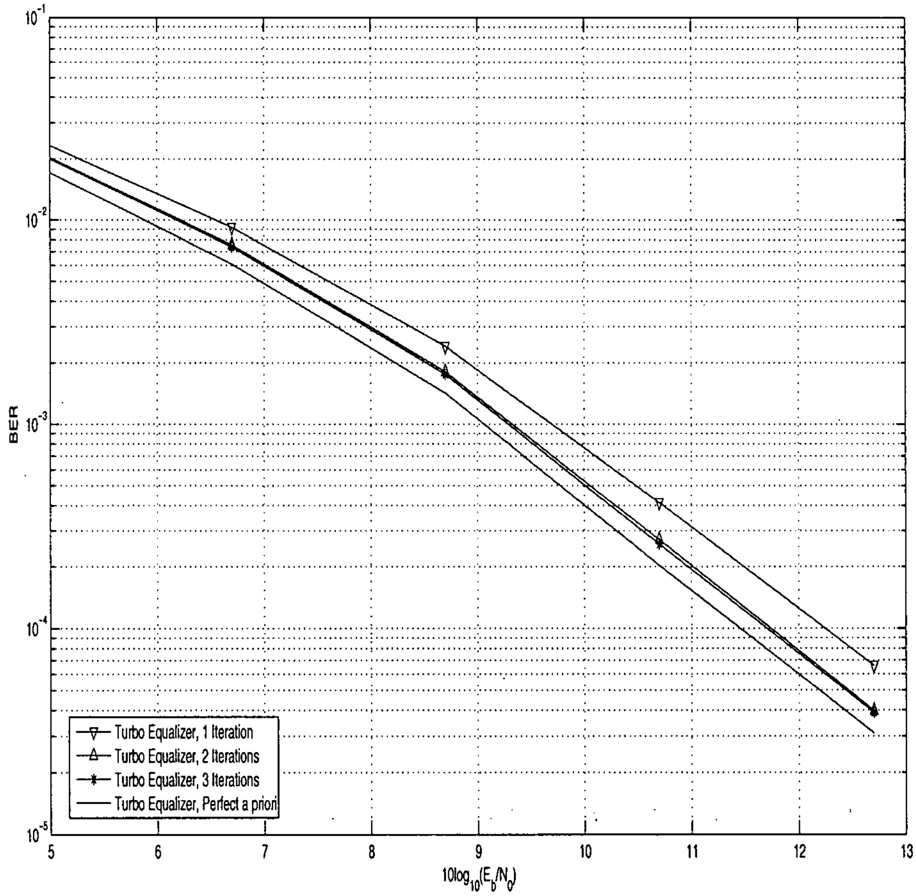

Figure 4.6: BER performance of frequency domain turbo equalizers for a BPSK DS-UWB system with spreading factor $N_s = 6$

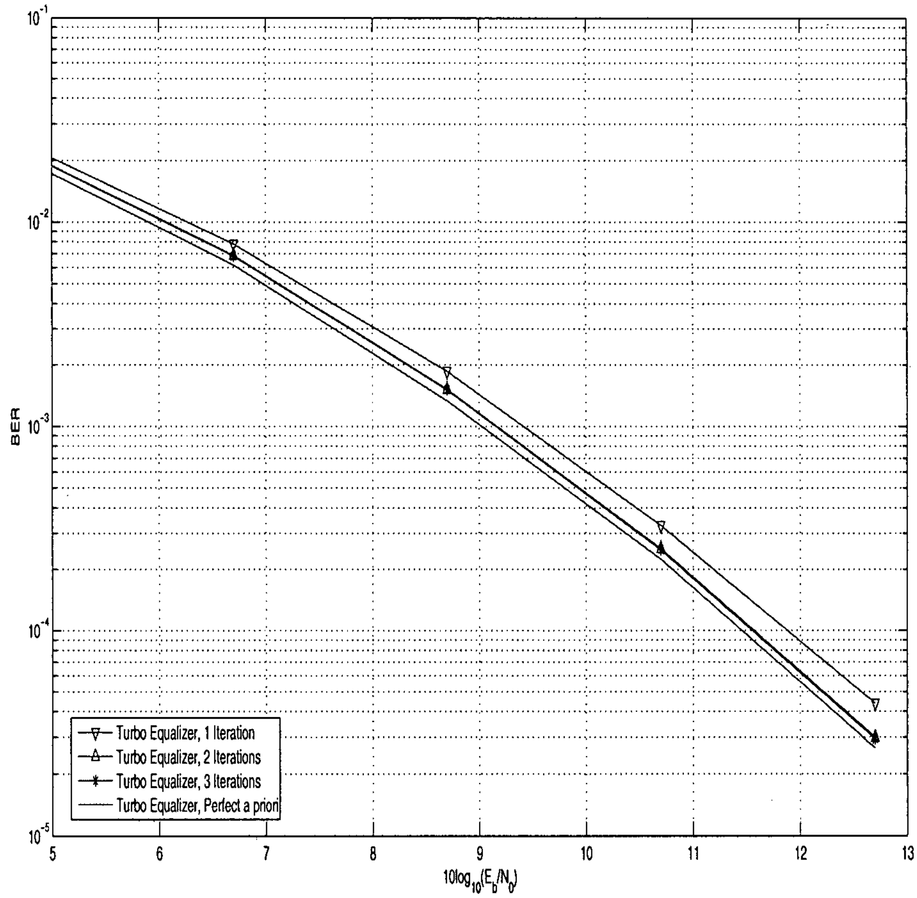

Figure 4.7: BER performance of frequency domain turbo equalizers for a BPSK DS-UWB system with spreading factor $N_s = 12$

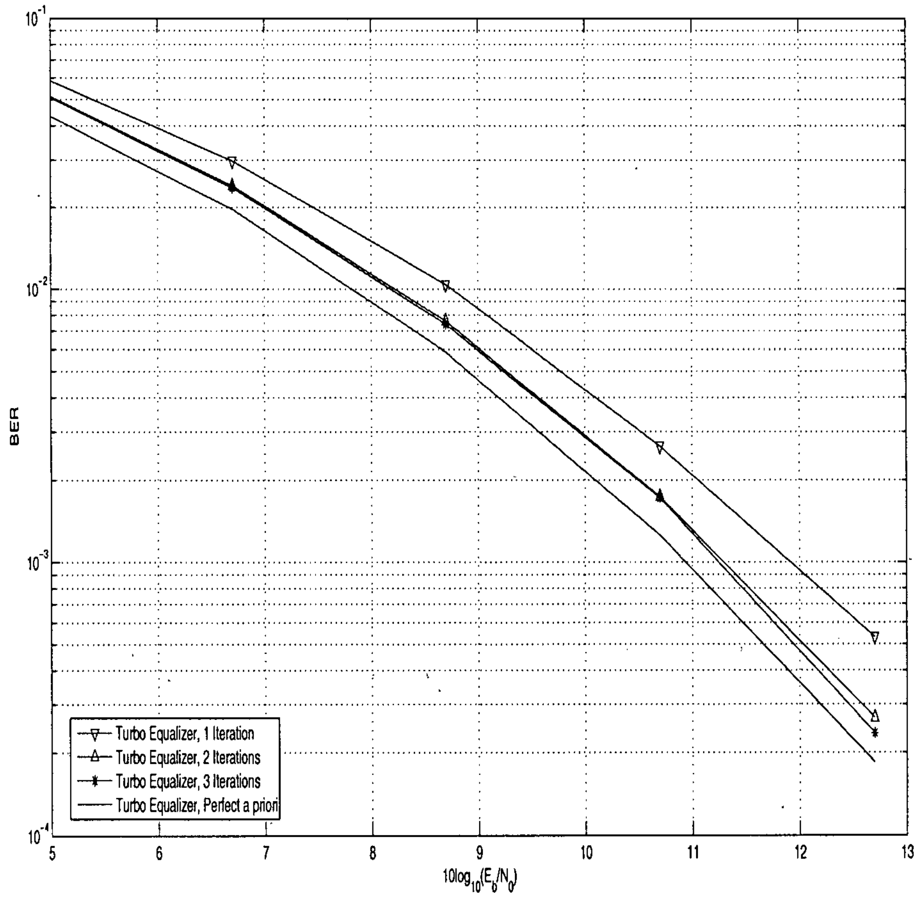

Figure 4.8: BER performance of frequency domain turbo equalizers for a 4BOK DS-UWB system with spreading factor $N_s = 6$

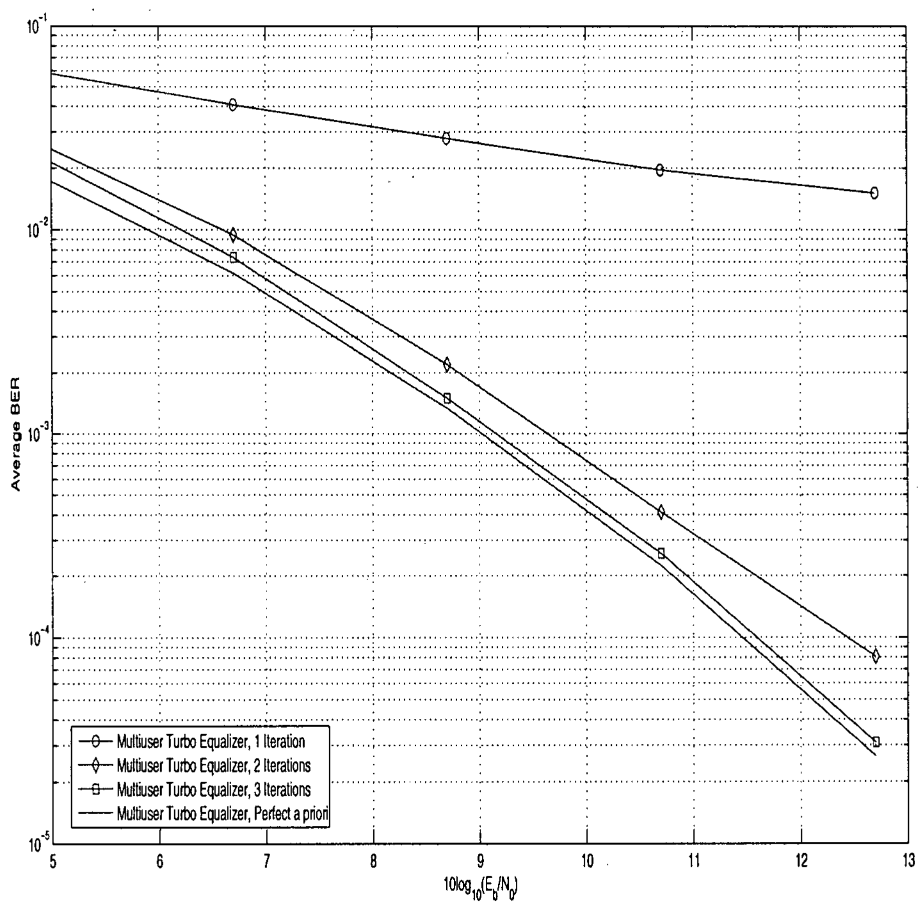

Figure 4.9: BER performance of frequency domain turbo equalizers for a 4-user BPSK DS-UWB system with spreading factor $N_s = 12$

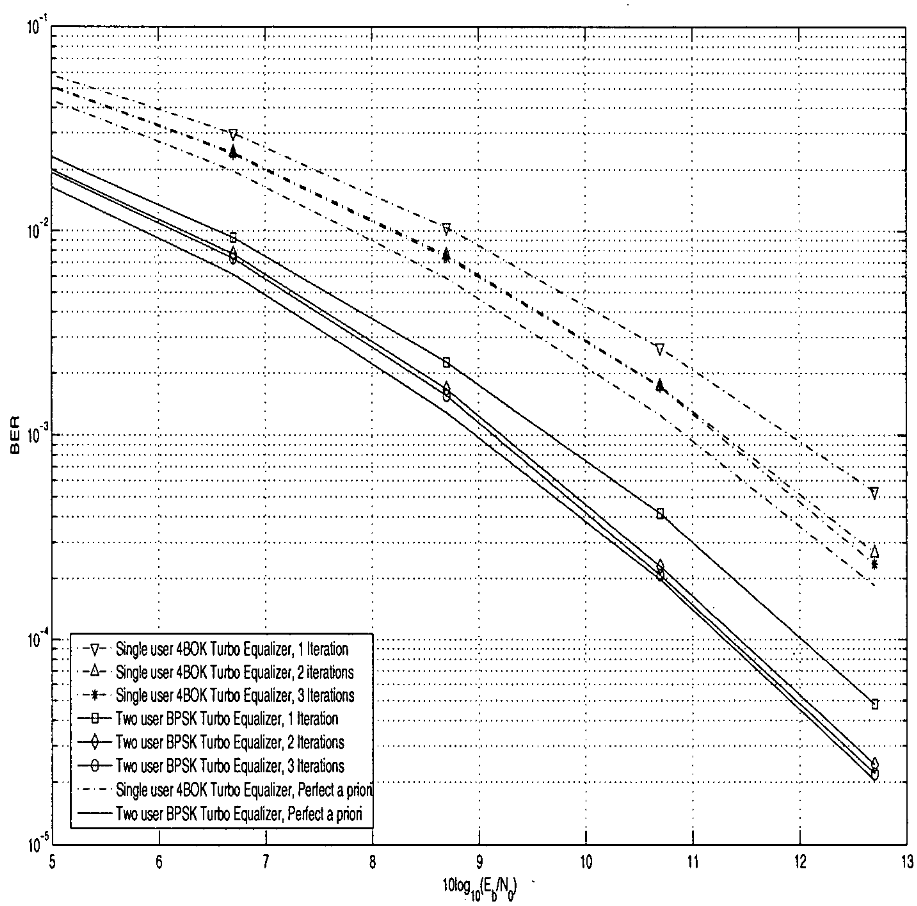

Figure 4.10: BER performance of frequency domain turbo equalizers for a 4BOK DS-UWB system with spreading factor $N_s = 6$, treating it as a 2-user BPSK DS-UWB system

Chapter 5

Conclusions

In this thesis, we considered frequency domain equalization for MBOK DS-UWB systems. The BER performances of various frequency domain equalization techniques were compared with that of time domain equalization techniques for single user systems. Symbol based frequency domain equalizers were first defined for BPSK DS-UWB systems. Later, it was shown that a single user 4BOK system can be seen as two-user BPSK system employing orthogonal codes. We then defined symbol based equalizers for a 4BOK system. We further analyzed the computational complexities of these equalization techniques for single user BPSK DS-UWB systems. Through simulations, it was shown that the frequency domain equalization techniques can offer better trade off between performance and complexity than time domain equalization techniques. The performance gain is more prominent for high data rate DS-UWB systems employing short spreading sequences over severely dispersive channels such as CM4.

We then considered multiuser DS-UWB systems. Iterative frequency domain multiuser detectors viz. SIC and PIC, were derived and their average BER performance was simulated. We then expressed a single user 4BOK system as a two user BPSK system and applied these multiuser receivers to detect transmitted bits. The performance of multiuser detectors was found to almost saturate after two decision feedback iterations. The performance of multiuser detection schemes for single user 4BOK system was found to be better compared to symbol based equalizers in chapter 2 but not as good as chip based equalizer.

We later considered coded DS-UWB systems. We proposed low complexity frequency domain turbo equalizers for single user BPSK and 4BOK DS-UWB systems and their performance was evaluated through simulations. We then considered coded multiuser DS-UWB system. Combining the single user frequency domain turbo equalization with soft interference cancelation, we derived a frequency domain multiuser turbo detector. We used this multiuser turbo detection technique to detect single user coded 4BOK system by considering it as a two-user BPSK system.

The performance improvement with use of turbo equalization techniques was found to be significant. Especially, in the case of multiuser systems, the performance gain was found to be very high. An improvement in performance was observed when multiuser turbo detector was used for single user 4BOK system, by considering it as a two-user BPSK system, compared to single user turbo equalizer.

5.1 Future Work

There are many interesting problems which can be pursued for future work.

- One of the main challenges for a UWB system is to mitigate the interference from narrowband systems [35]. Narrowband interference rejection techniques which operate in frequency domain have been studied in the literature for DS-CDMA systems [36]. These interference rejection schemes can be combined with the equalization and multiuser techniques presented in this thesis to improve the performance of DS-UWB systems by operating entirely in frequency domain.

- Recently, multi-input multi-output (MIMO) UWB systems are being considered to further increase the data rate of UWB systems. Frequency domain equalization for space-time block coded systems was studied in [37]. These equalization techniques can be applied for MIMO DS-UWB systems.

Bibliography

[1] L. Yang and G. B. Giannakis,"Ultra-wideband communications : an idea whose time has come," *IEEE Signal Process. Mag* , vol. 21, issue 6, pp.26-54, Nov 2004.

[2] J. Haartsen, M. Naghshineh, J. Inouye, 0. J. Joeressen, and W. Allen,"Bluetooth: vision, goals, and architecture," *Mobile Computing and Communications Review* , vol. 2, pp. 38-45, Oct. 1998.

[3] C.R. Buffler and P.O. Risman, "Compatibility Issues between Bluetooth and High Power Systems in the ISM Band," *Microwave Journal*, pp. 126131, July 2000.

[4] FCC Document 00-163: Revision of Part 15 of the Commission's Rules Regarding Ulra-Wideband Transmission Systems, ET Docket No 98-153, April 22, 2002.

[5] "DS-UWB physical layer submission to 802.15 Task Group 3a," *IEEE P802.15-04/0137r3*, July 2004.

[6] "Multi-band OFDM Physical Layer Proposal for IEEE 802.15 Task Group 3a," available on line www.multibandofdm.org.

[7] S. Oh-Soon, S. S. Ghazzemzadeh, L. J. Greenstein and V. Tarokh, "Performance evaluation of MB-OFDM and DS-UWB systems for wireless personal area networks," in *Proceedings of IEEE International Conference on Ultra-Wideband (ICU)*, Zurich, pp. 214-219, September 2005.

[8] K. Takizawa and R. Kohno, "Low-complexity rake reception and equalization for MBOK DS-UWB systems," *Global Telecommunications Conference, 2004. GLOBECOM '04. IEEE*, vol.2, pp.1249 - 1253, 29 Nov.-3 Dec. 2004.

[9] A. Parihar, L. Lampe, R. Schober and C. Leung,"Analysis of equalization for DS-UWB systems," in *Proceedings of IEEE International Conference on Ultra-Wideband (ICU)*, Zurich, pp.170-175, September 2005.

[10] Z. Lin, B. Premkumar and A.S. Madhukumar,"Tap selection based MMSE equalization for high data rate UWB communication systems," *IEEE International Symposium on Circuits and Systems, 2005. ISCAS 2005*, vol. 6, pp. 5421-5424, May 2005.

[11] M. E. Sahin and H. Arslan,"Inter-symbol interference in high data rate UWB communications using energy detector receivers ," in *Proceedings of IEEE International Conference on Ultra-Wideband (ICU)*, Zurich, pp.176-179, September 2005.

[12] D. Falconer, S. L. Ariyavisitakul, A. B. Seeyar and b. Eidson, "Frequency domain equalization for single-carrier broadband wireless systems," *IEEE Commun. Mag.*, vol 40, pp.58-66, Apr 2002.

[13] N. Benvenuto and S. Tomasin, "On the comparison between OFDM and single carrier modulation with DFE using a frequency-domain feedforward filter," *IEEE Trans. on Commun.*, vol 50, no. 6, pp. 947-955, June 2002

[14] Y. Ishiyama and T. Ohtsuki,"Performance evaluation of UWB-IR and DS-UWB with MMSE-frequency domain equalization," *Global Telecommunications Conference, 2004. GLOBECOM '04. IEEE*, vol 5, pp.3093-3097, 29 Nov.-3 Dec. 2004.

[15] H. Sato and T. Ohtsuki,"Performance evaluation of frequency domain equalization and channel estimation for direct sequence - ultra wideband (DS-UWB) system," *IEE Proceedings on Communications* , vol 135, issue 1, pp.93-98, 2 Feb. 2006.

[16] Y. Wang and X. Dong, "A time-division multiple-access SC-FDE system with IBI suppression for UWB communications," *IEEE Journal on Selected Areas in Communications*, vol. 24, issue 4, pp. 920-926, Apr. 2006.

[17] S. Tomasin and N. Benvenuto,"Frequency-domain interference cancellation and nonlinear equalization for CDMA systems," *IEEE Trans. Wireless Commun.*, vol 4, pp.2329-2339, Sept 2005.

[18] D. Falconer and S. L. Ariyavisitakul,"Broadband wireless using single carrier and frequency domain equalization," in *The 5th International Symposium on Wireless Personal Multimedia Communications, 2002.* , vol 1, pp.27-36, Oct 2002.

[19] Q. Li and L. A. Rusch, "Multiuser detection for DS-CDMA UWB in the homw environment," *IEEE Journal on Selected Areas in Communications*, vol. 20, no. 9, pp. 1701-1711, Dec. 2002.

[20] C. Douillard, M. Jezequel, C. Berrou, A. Picart, P. Didier, and A. Glavieux, "Iterative correction of intersymbol interference: Turbo equalization," *European Trans. Telecomm.*, vol. 6, pp. 507-511, Sept-Oct 1995.

[21] G. Bauch, H. Khorram, and J. Hagenauer, "Iterative equalization and decoding in mobile communications systems," in *The Second European Personal Mobile Communications Conference (2.EPMCC'Sr) together with 3. ITG-Fachtagung "Mobile Kommunikation"*, pp. 307-312, VDE/ITG, September/October 1997.

[22] A.F.Molisch, J.R. Foerster and M. Pendergrass,"Channel models for ultrawideband personal area networks ," in *IEEE Wireless Commun.*, vol.10, no.6, pp.14 - 21, Dec. 2003.

[23] A. Saleh and R. Valenzuela, "A Statistical Model for Indoor Multipath Propagation," *IEEE Journal on Selected Areas in Communications*, vol. SAC-5, no. 2, pp. 128-137, Feb. 1987.

[24] H. Sari, G. Karam and I. Jeanclaude, "Frequency domain equalization of mobile radio and terrestrial broadcast channels," *Global Telecommunications Conference, 1994. GLOBECOM '94. IEEE*, vol 5, pp.1-5, Nov.-Dec. 1994.

[25] T. Walzman and M. Schwartz,"Automatic equalization using the discrete Fourier domain," *IEEE Trans. Inform. Theory*, vol. IT-19, pp. 59-68, Jan. 1973.

[26] A. M. Chan and G. W. Wornell, "A class of block-iterative equalizers for intersymbol interference channels: Fixed channel results," *IEEE Trans. Commun.*, vol. 49, no. 11, pp. 1966-1976, Nov. 2001.

[27] F. Pancaldi and G. M. Vitetta, "Block channel equalization in the frequency domain," *IEEE Trans. Commun.*, vol. 53, no. 3, pp.463-471, March 2005.

[28] M. Tuchler and J. Hagenauer, "Turbo equalization using frequency domain equalizers," *Proc. of the Allerton Conference, Monticello, IL U.S.A*, Oct. 2000.

[29] C. M. Chang and K. C. Chen, "Frequency-domain approach to multiuser detection in DS-CDMA communications," *IEEE Commun. Letters*, vol. 4, no. 11, pp. 331-333, Nov. 2000.

[30] R. Koetter, A. C. Singer and M. Tuchler, "Turbo Equalization," *IEEE Signal Processing Mag.*, vol. 21, issue 1, pp.67-80, Jan 2004.

[31] M. Tuchler, A.C. Singer and R. Koetter, "Minimum mean squared error equalization using a priori information," *IEEE Trans. Signal Processing*, vol. 50, no. 3, pp.673-683, March 2002.

[32] C. Laot, R. L. Bidan and D. Leroux, "Low-complexity MMSE turbo equalization: a possible solution for EDGE," *IEEE Trans. Wireless Commun.*, vol. 4, no. 3, pp. 965-974, May 2005.

[33] B. Ng, D. Falconer, K. Kansanen and N. Veselinovic, "Frequency domain iterative methods for detection and estimation," *EURASIP 14th IST Mobile and Wireless Communications Summit, Dresden*, 19-23 June 2005.

[34] X. Wang and H. V. Poor, "Iterative (turbo) soft interference cancellation and decoding for coded CDMA," *IEEE Trans. Commun.*, vol. 47, no. 7, pp.1046-1061, July 1999.

[35] L. Zhao and A. M. Haimovich, "Performance of ultra-wideband communications in the prescence of interference," *IEEE Journal on Selected Areas in Communications*, vol. 20, no. 9, pp.1684-1691, Dec 2002.

[36] J. A. Young and J. S. Lehnert, "Analysis of DFT-based frequency excision algorithms for direct-sequence spread-spectrum communications," *IEEE Trans. Commun.*, vol. 46, no. 8, pp.1076-1087, Aug 1998.

[37] N. Al-Dhahir,"Single-carrier frequency-domain equalization for space-time block-coded transmissions over frequency-selective fading channels ," *IEEE Commun. Letters*, vol 5, issue 7, pp.304-306, July 2001.

Appendix A

Derivation of Frequency Domain Iterative Decision Feedback Equalizer

We assume that the frequency domain sequence $S(n)$ is independent and identically distributed with zero mean and variance σ_S^2. The problem is to minimize [26]

$$\begin{aligned} J^q &= E\left[|y[k] - s[k]|^2\right] \\ &= \frac{1}{N^2}\sum_{n=0}^{N-1} E\left[|Y^q(n) - S(n)|^2\right] \\ &= \frac{1}{N^2}\sum_{n=0}^{N-1} E\left[\left|W^q(n)R(n) + B^q(n)\hat{S}^{q-1}(n) - S(n)\right|^2\right] \end{aligned} \tag{A.1}$$

subject to constraint

$$\sum_{n=0}^{N-1} B^q(n) = 0 \tag{A.2}$$

To minimize J^q, its sufficient to minimize

$$J^q(n) = E\left[\left|W^q(n)R(n) + B^q(n)\hat{S}^{q-1}(n) - S(n)\right|^2\right] \tag{A.3}$$

for all $n = 0, 1, ..., N-1$.

The cost function to be minimized for each n, is given by

$$J_\beta^q(n) = E\left[|W^q(n)R(n) + B^q(n)\hat{S}^{q-1}(n) - S(n)|^2\right] + \beta\left(\frac{1}{N}\sum_{n=0}^{N-1} B^q(n)\right) \tag{A.4}$$

where β is the Lagrange multiplier to account for the constraint.

The correlation between sequences $S(n)$ and $\hat{S}^{q-1}(n)$ is assumed to be

$$\frac{E\left[S(n)\hat{S}^{q-1}(n')^*\right]}{\sigma_S^2} = \rho^q\delta(n-n') \tag{A.5}$$

This assumption holds true in most of the cases.

Now,

$$\begin{aligned}
J_\beta^q(n) &= E\left[|W^q(n)R(n) + B^q(n)\hat{S}^{q-1}(n) - S(n)|^2\right] + \beta\left(\frac{1}{N}\sum_{n=0}^{N-1} B^q(n)\right) \\
&= E\left[|(W^q(n)H(n)-1)S(n) + B^q(n)\hat{S}^{q-1}(n) + W^q(n)Z(n)|^2\right] \\
&\quad +\beta\left(\frac{1}{N}\sum_{n=0}^{N-1} B^q(n)\right) \\
&= E\left[|(W^q(n)H(n)-1)S(n) + B^q(n)\hat{S}^{q-1}(n)|^2\right] + N\sigma^2|W^q(n)|^2 \\
&\quad +\beta\left(\frac{1}{N}\sum_{n=0}^{N-1} B^q(n)\right) \\
&= \sigma_S^2|W^q(n)H(n)-1|^2 + (W^q(n)H(n)-1)B^q(n)^*\sigma_S^2\rho^q + \\
&\quad (W^q(n)H(n)-1)^*B^q(n)\sigma_S^2\rho^{q*} + \sigma_S^2|B^q(n)|^2 + N\sigma^2|W^q(n)|^2 \\
&\quad +\beta\left(\frac{1}{N}\sum_{n=0}^{N-1} B^q(n)\right)
\end{aligned} \tag{A.6}$$

Differentiating $J_\beta^q(n)$ w.r.t $B^q(n)$ and equating the derivative to zero, we obtain

$$B^q(n) = -(W^q(n)H(n)-1)\rho^q - \frac{1}{\sigma_S^2 N}\beta \tag{A.7}$$

Using the constraint $\sum_{n=0}^{N-1} B^q(n) = 0$, we get

$$
\begin{aligned}
\beta &= -\sigma_S^2 \rho^q \sum_{n=0}^{N-1} (W^q(n)H(n) - 1) \\
&= -\sigma_S^2 \rho^q N(\gamma^q - 1)
\end{aligned} \tag{A.8}
$$

where $\gamma^q = \frac{1}{N}\sum_{n=0}^{N-1} W^q(n)H(n)$

Substituting (A.8) in (A.7), we obtain

$$
B^q(n) = -\rho^q(W^q(n)H(n) - \gamma^q) \tag{A.9}
$$

Now, differentiating $J_\beta^q(n)$ w.r.t $W^q(n)$ and equating the derivative to zero, we obtain

$$
W^q(n) = \frac{\sigma_S^2 H(n)^*(1 + |\rho^q|^2\gamma^q)}{N\sigma^2 + \sigma_S^2(1 - |\rho^q|^2)|H(n)|^2} \tag{A.10}
$$

We can neglect the factor $1 + |\rho^q|^2\gamma^q$, as it is independent of n.

Therefore,

$$
W^q(n) = \frac{\sigma_S^2 H(n)^*}{N\sigma^2 + \sigma_S^2(1 - |\rho^q|^2)|H(n)|^2} \tag{A.11}
$$

Appendix B

Derivation of Frequency domain MMSE Turbo Equalizer

The cost function to be minimized for each n, is given by [32]

$$J_\beta(n) = E\left[|W(n)R(n) + B(n)\bar{S}(n) - S(n)|^2\right] + \beta\left(\frac{1}{MN_s}\sum_{n=0}^{MN_s-1} B(n)\right) \tag{B.1}$$

where β is the Lagrange multiplier.

Now,

$$\begin{aligned}
J_\beta(n) &= E\left[|W(n)R(n) + B(n)\bar{S}(n) - S(n)|^2\right] + \beta\left(\frac{1}{MN_s}\sum_{n=0}^{MN_s-1} B(n)\right) \\
&= E\left[|(W(n)H(n) - 1)S(n) + B(n)\bar{S}(n) + W(n)Z(n)|^2\right] \\
&\quad +\beta\left(\frac{1}{MN_s}\sum_{n=0}^{MN_s-1} B(n)\right) \\
&= E\left[|(W(n)H(n) - 1)S(n) + B(n)\bar{S}(n)|^2\right] + MN_s\sigma^2|W(n)|^2 \\
&\quad +\beta\left(\frac{1}{MN_s}\sum_{n=0}^{MN_s-1} B(n)\right) \\
&= \sigma_S^2|W(n)H(n) - 1|^2 + \sigma_{\bar{S}}^2[|B(n)|^2 + (W(n)H(n) - 1)B(n)^* \\
&\quad +(W(n)^*H(n)^* - 1)B(n)] + MN_s\sigma^2|W(n)|^2 + \beta\left(\frac{1}{MN_s}\sum_{n=0}^{MN_s-1} B(n)\right)
\end{aligned} \tag{B.2}$$

Differentiating $J_\beta(n)$ w.r.t $B(n)$ and equating the derivative to zero, we obtain

$$B(n) = -(W(n)H(n) - 1) - \frac{1}{\sigma_{\bar{S}}^2 MN_s}\beta \tag{B.3}$$

Using the constraint $\sum_{n=0}^{MN_s-1} B(n) = 0$, we get

$$\begin{aligned} \beta &= -\sigma_{\bar{S}}^2 \sum_{n=0}^{MN_s-1} (W(n)H(n) - 1) \\ &= -\sigma_{\bar{S}}^2 MN_s(\mu - 1) \end{aligned} \tag{B.4}$$

where $\mu = \frac{1}{MN_s}\sum_{n=0}^{MN_s-1} W(n)H(n)$

Substituting (B.4) in (B.3), we obtain

$$B(n) = \mu - W(n)H(n) \tag{B.5}$$

Now, differentiating $J_\beta(n)$ w.r.t $W(n)$ and equating the derivative to zero, we obtain

$$W(n)^* = \frac{H(n)\left[\sigma_S^2 - \sigma_{\bar{S}}^2\mu\right]}{(\sigma_S^2 - \sigma_{\bar{S}}^2)|H(n)|^2 + MN_s\sigma^2} \tag{B.6}$$

We define

$$\tilde{W}(n) = \frac{H(n)^*}{(\sigma_S^2 - \sigma_{\bar{S}}^2)|H(n)|^2 + MN_s\sigma^2} \tag{B.7}$$

$$\tilde{\mu} = \frac{1}{MN_s}\sum_{n=0}^{MN_s-1} \tilde{W}(n)H(n) \tag{B.8}$$

Then, equation (B.6) is equivalent to

$$W(n) = \lambda\tilde{W}(n) \tag{B.9}$$

where

$$\lambda = \sigma_S^2 - \sigma_{\bar{S}}^2\mu \tag{B.10}$$

Therefore,

$$\mu = \lambda\tilde{\mu} \tag{B.11}$$

Using (B.10) and (B.11), we obtain

$$\lambda = \frac{\sigma_S^2}{1 + \sigma_{\bar{S}}^2 \tilde{\mu}} \tag{B.12}$$

Substituting (B.5), (B.9) in (4.5), we obtain

$$J(n) = \frac{|H(n)|^2 \lambda}{(\sigma_S^2 - \sigma_{\bar{S}}^2)|H(n)|^2 + MN_s\sigma^2}\left[\lambda + 2\sigma_{\bar{S}}^2 - 2\sigma_S^2\right] + \mu^2\sigma_{\bar{S}}^2 - 2\mu\sigma_{\bar{S}}^2 + \sigma_S^2 \tag{B.13}$$

Using (B.9)-(B.12) and (4.3), we obtain

$$\begin{aligned}
J &= \frac{1}{(MN_s)^2}\sum_{n=0}^{MN_s-1} J(n) \\
&= \frac{1}{(MN_s)^2}\sum_{n=0}^{MN_s-1} E\left[|W(n)R(n) + B(n)\bar{S}(n) - S(n)|^2\right] \\
&= \frac{1}{MN_s}\left(\sigma_S^2 - 2\sigma_S^2\mu + \mu(\lambda + \mu\sigma_{\bar{S}}^2)\right) \\
&= \frac{1}{MN_s}\left(\sigma_S^2 - 2\sigma_S^2\mu + \mu\sigma_S^2\right) \\
&= \frac{1}{MN_s}\sigma_S^2(1-\mu)
\end{aligned} \tag{B.14}$$

Thus, for MMSE filtering

$$E(|y[k] - s[k]|^2) = \frac{1}{MN_s}\sigma_S^2(1-\mu) \tag{B.15}$$